

Sveinung Grov

Electrochemical Energy Storage for an HVDC transmission system connected to an offshore wind farm

Bachelor's thesis in Electric Power Engineering

Supervisor: Ian Norheim

May 2022

NTNU
Norwegian University of Science and Technology
Faculty of Information Technology and Electrical Engineering
Department of Electric Power Engineering

Sveinung Grov

Electrochemical Energy Storage for an HVDC transmission system connected to an offshore wind farm

Bachelor's thesis in Electric Power Engineering
Supervisor: Ian Norheim
May 2022

Norwegian University of Science and Technology
Faculty of Information Technology and Electrical Engineering
Department of Electric Power Engineering

The title of the thesis: <i>Electrochemical Energy Storage for an HVDC transmission system connected to an offshore wind farm</i>	Date: 2022-05-20
	Number of pages: 84
	Master's thesis: <input type="checkbox"/> Bachelor's thesis: <input checked="" type="checkbox"/>
Name: Sveinung Grov	
Supervisor: Ian Norheim, NTNU	
External professional contacts / supervisors: Kamran Torki Sharifabadi, client representative, Equinor	

Abstract:

The objective of this thesis, written for Equinor, is to review and assess solutions for electrochemical energy storage for an HVDC transmission system connected to an offshore wind farm. Both with regards to the selection of the electrochemical storage technology, the converter technology for connection to the system and the point of connection to the HVDC system.

This Bachelor thesis is based upon a literature review. Literature is reviewed to identify the power system stability services needed, to identify the dimensioning criteria, and to identify possible technological solutions and the availability of these. Furthermore, are the identified solutions assessed by the student. Based on the literature review and the assessments, recommendations are provided and justified.

The lithium-ion battery technology is identified to be the most promising technology for electrochemical energy storage, due to its technical properties and proven result from deployments in large-scale power system stabilizing energy storage plants. The sub-category lithium iron phosphate (LFP) is selected as the recommended battery chemistry. This to reduce the reliance on scarce minerals and as the LFP deployment is considered to increase in the years to come.

It is recommended to use a commercially available BESS solution connected to the AC grid side, as these are both available and have proven their functionalities in large-scale plants which exceeds the need identified in this thesis. This will have less project risks and probably a lower cost. The usage of larger BESS units is interesting and should be followed up closely in the years to come. Large scale HVDC-MMC-BESS's may be a competitive option if a significant amount of the traditional power sources is to be displaced by inverter-based resources in the bulk power system.

Keywords:

HVDC, BESS, MMC, VSC
Electrochemical Energy Storage
Ancillary Services
Primary and Secondary Reserves



(sign.)

Sammendrag

Formålet med denne oppgaven, skrevet for Equinor, er å gjennomgå og vurdere løsninger for elektrokjemisk energilagring for et HVDC transmisjonssystem tilkoblet en offshore havvindpark. Både med hensyn på å velge teknologi for elektrokjemisk energilagring, omformerteknologi for tilkobling til systemet og punktet for tilkobling til HVDC-systemet.

Denne Bachelor-oppgaven er basert på et litteraturstudium. Litteratur er gjennomgått for å identifisere de nødvendige funksjonalitetene for kraftsystembalansering, for å identifisere dimensjonerende kriterier og for å identifisere tekniske løsninger og tilgjengeligheten av disse. Videre så er de identifiserte tekniske løsningene vurdert av studenten. Basert på litteraturstudiet og vurderingene, så er anbefalinger blitt gitt og begrunnet.

Lithium-ion er den batteriteknologien som er identifisert til å være den mest lovende teknologien for elektrokjemisk energilagring. Både med bakgrunn i de tekniske egenskapene til lithium-ion, men også med bakgrunn i resultatene bevist i flere ferdigstilte prosjekter, der lithium-ion er anvendt i stor-skala energilagringssystemer for nettstabilisering. Underkategorien lithium-iron-phosphate (LFP) er valgt som anbefalt batteriteknologi. Dette for å redusere avhengigheten av knappe eller sjeldne mineraler, men også pga. at LFP er ansett å ville utgjøre en økende andel av lithium-ion batteriteknologiene satt i drift i de kommende årene.

Det er anbefalt å bruke en kommersielt tilgjengelig BESS pakkelsning, tilkoblet AC-nettsiden av HVDC-omformeren på land. Både siden BESS-løsningene er tilgjengelige på markedet, men også med bakgrunn i bevist resultat fra storskala energilagring som overgår behovet identifisert i denne oppgaven. Dette vil ha en lavere prosjektrisiko og trolig en lavere kostnad, enn alternativene. Bruken av større BESS-enheter er interessant og bør følges opp tett i årene som kommer. Storskala HVDC-MMC-BESS-enheter kan være et konkurransedyktig alternativ dersom en stor andel av de tradisjonelle kraftkildene anses å bli fortrent av inverter-baserte ressurser i transmisjonsnettet.

Preface

This Bachelor thesis constitutes the final assignment in my study program in Electric Power Engineering at NTNU and is submitted in May 2022. It has been instructive years ended with an interesting and captivating assignment.

This thesis is written by Sveinung Grov. The work started January 10th, 2022, and the thesis were submitted on May 20th, 2022.

The thesis is written for Equinor under guidance from both Equinor and NTNU.

I am very grateful for the opportunity to write this thesis and I would specially thank Ian Norheim, NTNU and Kamran Torki Sharifabadi, Equinor for their guidance, knowledge, and encouragement.

Sveinung Grov, May 20th, 2022

Table of Content

- 1 Introduction 1
 - 1.1 Background..... 1
 - 1.2 Objectives and problem statement..... 2
 - 1.3 Scope of Work (SoW) and limitations 2
 - 1.4 Thesis Outline..... 4
- 2 Literature review 5
 - 2.1 Power System Stability..... 5
 - 2.1.1 Ancillary Services and Traditional Services 6
 - 2.1.2 Inertia in the Bulk Power System (BPS)..... 7
 - 2.1.3 Primary Frequency Response (PFR) and Secondary Control 9
 - 2.1.4 Renewable Energy Sources (RES)..... 12
 - 2.1.5 Inverter-Based Resources (IBR’s) 13
 - 2.1.6 Fast Frequency Response (FFR) 16
 - 2.1.7 Grid-Forming (GFM) Control Strategies 17
 - 2.1.8 Geographical Considerations 19
 - 2.2 Electrochemical Energy Storage Technologies 21
 - 2.2.1 Batteries..... 22
 - 2.2.2 Lithium-ion..... 23
 - 2.2.3 Sodium-sulfur..... 28
 - 2.2.4 Flow batteries 31
 - 2.2.5 Lead-Acid..... 34
 - 2.2.6 Summary of the Electrochemical Review 36
 - 2.2.7 State of Charge (SoC) 37
 - 2.3 HVDC Technology & HVDC Systems 38
 - 2.3.1 Line Commutated Converters (LCC)..... 38
 - 2.3.2 Voltage Source Converters (VSC) 39
 - 2.3.3 Modular Multilevel Converters (MMC) 40
 - 2.3.4 Available HVDC solutions in the market 42
 - 2.3.5 Offshore Wind HVDC Reference Projects 43
 - 2.4 Battery Energy Storage Systems (BESS) 44

2.4.1	BESS Technologies.....	45
2.4.2	Available BESS solutions in the market	46
2.4.3	Large-Scale Grid Stabilizing BESS Reference Projects	48
2.5	BESS for HVDC.....	49
2.5.1	BESS connected to the DC link	49
2.5.2	BESS connected to the AC grid side of the onshore Converter.....	52
3	Assessment of Solutions.....	53
3.1	Dimensioning Criteria's	53
3.2	Electrochemical Storage Technology	56
3.3	BESS connection to the HVDC system.....	59
3.3.1	Case 1: Commercially available BESS connected to the AC grid.....	59
3.3.2	Case 2: MMC-BESS connected to the DC-link of the HVDC system	62
3.3.3	Case 3: MMC-BESS connected to the onshore AC grid	67
4	Discussion	70
5	Conclusion.....	75
6	Further Work	76
	References	78

List of Tables

Table 2.1:	Summary of reviewed data for lithium-ion batteries	25
Table 2.2:	Summary of reviewed data for sodium-sulfur batteries	29
Table 2.3:	Summary of reviewed data for flow batteries	32
Table 2.4:	Summary of reviewed data for lead-acid batteries	35
Table 2.5:	Summary of the review in chapter 2.2, for comparison purpose	36
Table 2.6:	Available HVDC VSC products in the market, [34, 35, 36]	42
Table 2.7:	Commercially available BESS products in the market, [45, 46, 47, 48, 49, 50, 51, 52, 53, 54, 55, 56, 57, 58, 59]	46
Table 3.1:	Summary of the review in chapter 2.2, colored to highlight pros & cons	57

List of Figures

Figure 1.1:	Block diagram of an HVDC scheme where a BESS is connected to the DC-link of the HVDC	3
Figure 1.2:	Block diagram of an HVDC scheme where a BESS is connected to the AC grid side of the onshore converter	4
Figure 2.1:	Control Continuum showing overlapping services. Figure from [1]	6
Figure 2.2:	A bulk power system containing synchronous generators synchronized at the same frequency due to electromagnetic forces, represented by chains. Figure adapted from [2]	7
Figure 2.3:	Recovery from a contingency event where both inertia and PFR contributed to the recovery	10
Figure 2.4:	Bulk Power System of today and in the future, with a higher RES penetration	12
Figure 2.5:	Illustration of Inverter Based Resources (IBR's)	13
Figure 2.6:	The properties of IBR's, GFL IBR's and GFM IBR's put into a figure for comparison	15
Figure 2.7:	Recovery from a contingency event where both low inertia and FFR contributed to the recovery	16
Figure 2.8:	Illustration of the $P - f$ ($P - \omega$) and $Q - V$ relationships for GFL IBR's	17
Figure 2.9:	Illustration of the $P - f$ ($P - \omega$) and $Q - V$ relationships for GFM IBR's ...	18
Figure 2.10:	Wide area synchronous grid. Source: Wikimedia Commons [9]	19
Figure 2.11:	Electrochemical cell. Source: Wikimedia Commons [13]	21
Figure 2.12:	Ragone plot showing the properties for some common battery technologies. Source: Wikimedia Commons [14]	22
Figure 2.13:	LFP cells connected in parallel and series. Source: Wikimedia Commons [18]	24
Figure 2.14:	Charge-discharge diagram for a lithium-air battery. Source: Wikimedia Commons [22]	26
Figure 2.15:	Sodium-sulfur battery. Source: Wikimedia Commons [23]	28
Figure 2.16:	Redox Flow Battery. Source: Wikimedia Commons [25]	31

Figure 2.17:	1 MW 4 MWh Containerized vanadium flow battery. Source: Wikimedia Commons [26]	33
Figure 2.18:	A traditional lead-acid car battery. Source: Wikimedia Commons [27]	34
Figure 2.19:	Illustrating an HVDC scheme or HVDC transmission system, including converter transformers	38
Figure 2.20:	Illustrating the active and reactive power flow for an LCC-HVDC	39
Figure 2.21:	Illustrating the active and reactive power flow for a VSC-HVDC	39
Figure 2.22:	Illustrating the active and reactive power flow for an MMC-HVDC	40
Figure 2.23:	Principle for a Modular Multilevel Converter. Source: Wikimedia Commons [32]	41
Figure 2.24:	Modular Multilevel Converter. Submodule states. Source: Wikimedia Commons [33]	41
Figure 2.25:	Showing a picture of the Tehachapi Energy Storage Project (TSP). Source: Wikimedia Commons [44]	44
Figure 2.26:	Single-stage and two-stage VSC for BESS application	45
Figure 2.27:	Block diagram of the HVDC scheme and BESS used in the reviewed Master Thesis. Recreated based on Figure 1.1 in [42]	50
Figure 2.28:	Single-line diagram of the HVDC scheme and BESS connection, used in the reviewed Master Thesis. Recreated based on Figure 1.1 in [43]	52
Figure 3.1:	Block diagram showing the point of connection to the system	59
Figure 3.2:	Block diagram that illustrates several BESS's connected to the AC-grid side	60
Figure 3.3:	Block diagram that illustrates several BESS's connected to the AC-grid side	61
Figure 3.4:	Single-line diagram of an MMC-BESS connected to the DC-link of the HVDC system	62
Figure 3.5:	Single-line diagram of an offshore windfarm project developed in three project phases, where an MMC-BESS is connected to the DC-link for one of the HVDC's	64
Figure 3.6:	Single-line diagram of an MMC-BESS connected to the DC-link of an HVDC and where an external onshore contingency event occurs when the wind farm operates at maximum output.....	65

Figure 3.7:	Single-line diagram of a multiterminal HVDC scheme with “hybrid cables” and an MMC-BESS connected to the DC-link.....	66
Figure 3.8:	Single-line diagram of the HVDC scheme and MMC-BESS connection	67
Figure 3.9:	Single-line diagram of three HVDC schemes and the MMC-BESS connection	68
Figure 3.10:	Single-line diagram of three HVDC schemes and two or more MMC-BESS’s	69

Abbreviations

BES	=	Battery Energy Storage
BESS	=	Battery Energy Storage System
BPS	=	Bulk Power System
CAES	=	Compressed Air Energy Storage
DAB	=	Dual Active Bridge
DPS	=	Dynamic Performance Study
EES	=	Electrochemical Energy Storage
ESS	=	Energy Storage System
FBES	=	Flow Battery Energy Storage
FES	=	Flywheel Energy Storage
FFR	=	Fast Frequency Response
GFL	=	Grid-Following
GFM	=	Grid-Forming
HVAC	=	High Voltage Alternating Current
HVDC	=	High Voltage Direct Current
IBR	=	Inverter Based Resources
IGBT	=	Insulated Gate Bipolar Transistor
IP	=	Intellectual Property
LCC	=	Line Commutated Converters
LFP	=	Lithium Iron Phosphate
MMC	=	Modular Multilevel Converter
NCA	=	Nickel Cobalt Aluminum
NCS	=	Norwegian Continental Shelf
NMC	=	Nickel Manganese Cobalt
PCC	=	Point of Common Coupling
PFR	=	Primary Frequency Response
PHS	=	Pumped Hydro Storage
PWM	=	Pulse-Width Modulation
RES	=	Renewable Energy Sources
SCADA	=	Supervisory Control And Data Acquisition
SCES	=	Supercapacitor Energy Storage
SMES	=	Superconducting Magnetic Energy Storage
UFLS	=	Under Frequency Load Shedding
VSC	=	Voltage Source Converter
2L-VSC	=	Two-Level Voltage Source Converter
3L-VSC	=	Three-Level Voltage Source Converter
VSM	=	Virtual Synchronous Machine

1 Introduction

1.1 Background

As a direct consequence of the global warming and the climate change, larger parts of the global energy sources are desired to be shifted from fossil fueled energy sources to renewable energy sources (RES).

This shift in energy sources comes with some new considerations.

Conventional energy sources, such as hydroelectrical power plants, nuclear power plants, fossil fueled power plants, consisting of gas- and steam turbines, do all have a common denominator – they have spinning synchronous generators. These spinning generators will work as a spinning reserve providing inertia, which as per today is one of the main contributors for grid stabilization.

When integrating large amounts of RES to an existing grid, the grid stabilization must be considered and maintained. RES, such as solar energy systems and wind energy systems do not have spinning generators providing inertia, as power electronic components are connected in-between the source and the grid. However, modern inverter-based resources (IBR's) do provide other functionalities and possibilities with regards to grid stabilization.

The background for this Bachelor thesis is an assignment received from the Equinor, which is a large Norwegian energy company. Equinor is well known for its activities in the oil- and gas industry and have the responsibility for significant amounts of the oil- and gas production on the Norwegian Continental Shelf (NCS). Furthermore, Equinor has a large portfolio of offshore electrification projects and projects where RES will be integrated into the onshore bulk power system (BPS). This RES integration will be the background for this thesis.

A power system of an offshore wind farm connected to shore via an HVDC transmission system is considered. Energy storage in the form of electrochemical battery storage shall be connected to the system in order to provide services of primary and secondary reserves for power system stability (which ancillary services can be provided with a battery storage).

1.2 Objectives and problem statement

The main objectives for this project and this thesis will be to review and assess different battery technologies, converter topologies, possible point of connection to the HVDC system and finally to recommend one or more possible solutions to provide ancillary services of primary and secondary reserves. The end goal is to have an optimal battery technology and an optimal point of connection to the system.

How to connect an electrochemical energy storage to an HVDC transmission system for an offshore wind farm, to provide onshore power system stability?

1.3 Scope of Work (SoW) and limitations

As NTNU wants to avoid confidential Bachelor theses and as the student were strongly recommended to create an open report, it has been decided to not reveal any project specific details in this work. This may lead to some constraints in the work process, but it does also give rise to some opportunities.

Instead of basing the project on given project data and requirements, literature is assessed, both to identify the need and the solution.

This gives the opportunity to review traditional power system stability services, the impact of high RES penetration, geographical considerations, the size of the reserve needed, in addition to the literature review with respect to solutions.

This approach gives the reader an introduction to traditional power system stabilization, an in-depth understanding of the pros and cons that comes with RES integration, before finally reviewing and assessing solutions for electrochemical energy storage for an HVDC system.

Furthermore, this approach gives data which can be used in the decision-making processes for multiple HVDC RES projects, as external factors and geographical impacts are highlighted.

Electrochemical energy storage technologies will be reviewed and assessed. The focus will be on the grid scale application and the physical properties required for such a usage. Any recommendation with regards to storage technology will be justified and the parameters for selection will be highlighted. Both technological available solutions, commercially available solutions and promising technologies will be assessed.

Battery Energy Storage Systems (BESS's) will be reviewed and assessed. The focus will be on the grid scale application and the possibilities with regards to connection to the HVDC system or to the onshore AC grid side. Furthermore, both technological feasible solutions and commercially available solutions will be assessed. Any recommendation will be justified.

It is decided to not do any simulations in this project. A simulation model could have been created by using digital tools like MATLAB Simulink, PSCAD or similar. However, this simulation would have required simplifications due to the complexity of modern HVDC's and BESS systems, and due to the lack of proprietary data. This simplified model would have shown principles but would not have given any clear result with regards to efficiency and cost, which makes the backbone for the decision making in this thesis.

Furthermore, this thesis is limited to the concept selection and not a detail engineering of any solution. The focus has exclusively been on the literature review and the assessment of data. As a requirement from Equinor is that the decision making should be based on fresh literature from after 2016, the focus has been on identifying such literature and any other task would have impacted this work and the quality in the assessments.

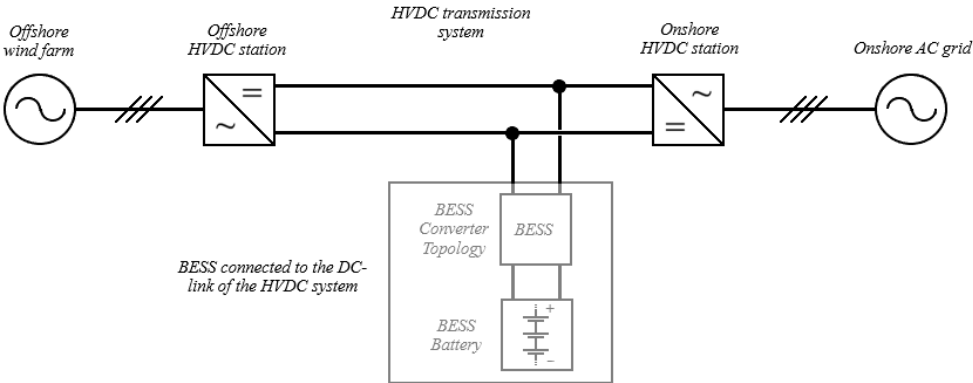


Figure 1.1: Block diagram of an HVDC scheme where a BESS is connected to the DC-link of the HVDC

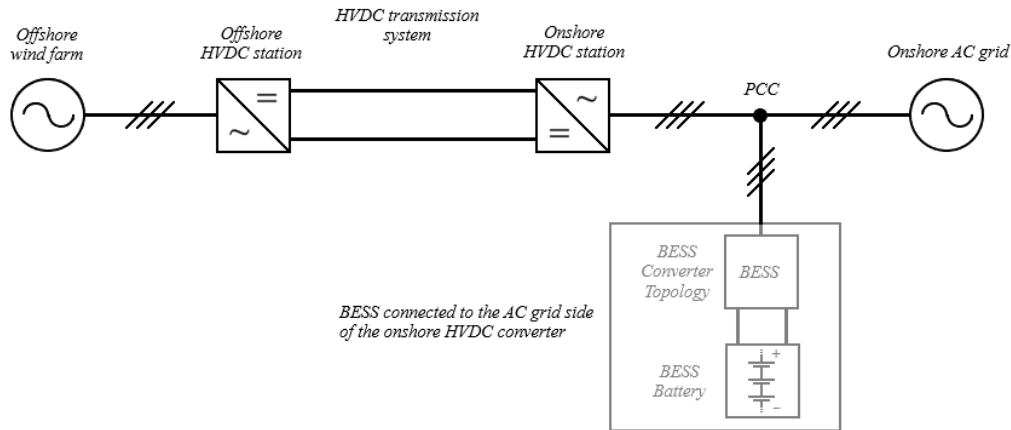


Figure 1.2: Block diagram of an HVDC scheme where a BESS is connected to the AC grid side of the onshore converter

1.4 Thesis Outline

This report starts with an introduction part, explaining the background for this thesis, the objectives and the problem statement, and an outline of the thesis. Followed by a larger chapter for the literature review, which will make up most of the content of the report. This chapter aims to enlighten the reader in an orderly manner, so that the reader first gets an impression of the need and reasons before the solutions and options are reviewed. This is followed by a chapter for assessments of solutions, which mainly will be based on the harvested data presented in the literature review chapter. Chapter for discussions and conclusions are furthermore built on top of the review and assessment chapters. Identified needs with regards to further work are presented in the last chapter.

- Chapter 1: Introduction
- Chapter 2: Literature review
- Chapter 3: Assessment of solutions
- Chapter 4: Discussion
- Chapter 5: Conclusion
- Chapter 6: Further work
- References

2 Literature review

In this chapter literature are reviewed with the sole purpose of creating a solid fundament for the assessments to be performed in chapter 3.

The literature review starts with a review of power system stability services, traditionally services and the disadvantages and advantages of increasing the amount of inverter-based resourced in the bulk power system.

This is followed by a review of electrochemical energy storage technologies, where the most promising technologies has been selected. An extensive search after newer high quality comparison studies for grid-scale electrochemical energy storage technologies has been performed. The literature review in this thesis is mainly built on top of this identified material.

HVDC and BESS technologies are reviewed, and commercially available solutions are identified. As already mentioned, only the harvested data are presented in chapter 2 and the assessments are to be performed in chapter 3 based upon the data in chapter 2.

2.1 Power System Stability

To get the required understanding about power system stability, ancillary services, primary reserves, secondary reserves and the needs and requirements for the system assessed in this thesis – the traditional services for power system stability must first be fully understood.

This chapter aims to give the reader an introduction to traditional power system stability mechanisms, definitions and terms used, the implications that renewable energy sources and inverter-based resources are causing and how these resources could be utilized for grid stabilizing services. Frequency stability is more thorough described than voltage stability, as frequency stability and the active power needed, is the dimensioning criteria for the reserve.

Furthermore, this chapter will give answers to dimensioning considerations and geographical considerations that are relevant for the assessments in the subsequent assessment chapters.

2.1.1 Ancillary Services and Traditional Services

Ancillary services are imperative with regards to ensuring a stable and reliable grid operation. Two main indicators for a healthy grid operation, are frequency stability and voltage stability, where the frequency is closely connected to the supply and demand of active power and where the voltage stability is closely tied to the reactive power.

It exists several types of services, where some services may slow the direct consequence of a contingency event, i.e., slow the rate of frequency decline, some services may stop the frequency decline and stabilize the frequency and some services are bringing the frequency back to nominal predefined values [1]. These services are grouped into different categories based upon their purpose, response time and are mainly named and categorized based upon their traditional grid stabilizing technology [1].

In the following subsequent chapters, the most important services will be reviewed.

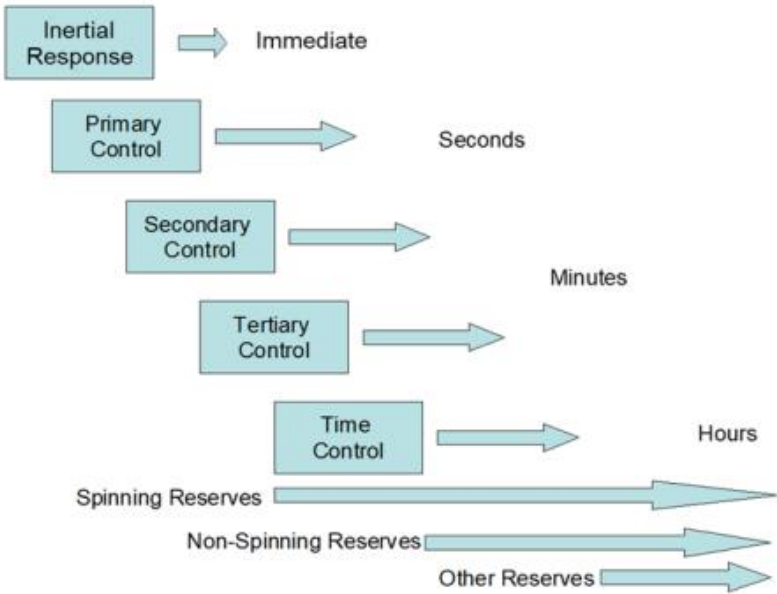


Figure 2.1: Control Continuum showing overlapping services. Figure from [1]

2.1.2 Inertia in the Bulk Power System (BPS)

Inertia is in physical terms well known to be the tendency of an object in motion to remain in motion. Moreover, it is in more practical terms, the reason for a car to keep its motion, even if the driver removes his/her foot from the gas pedal and furthermore the reason that a car or a bicycle must have brakes to slow down and stop. Spinning objects have rotational inertia and this applies to electromechanical equipment like a power generator [2].

With regards to inertia in the power system, the term inertia refers to the kinetic energy stored in spinning synchronous generators and the inertial response these are causing [2].

Inertia has been, and in many cases still are, an important grid service for power system stability. In an interconnected bulk power system, it may be hundreds or even thousands of spinning generators that are operating synchronous at the same frequency. This frequency is determined by how fast the mentioned synchronous generators spins. Electromagnetic forces ensures that these generators are rotating in lock step at the exact same frequency [2]. This can be illustrated in figure 2.2 where the chains are representing the electromagnetic forces for each individual synchronous generator [2].

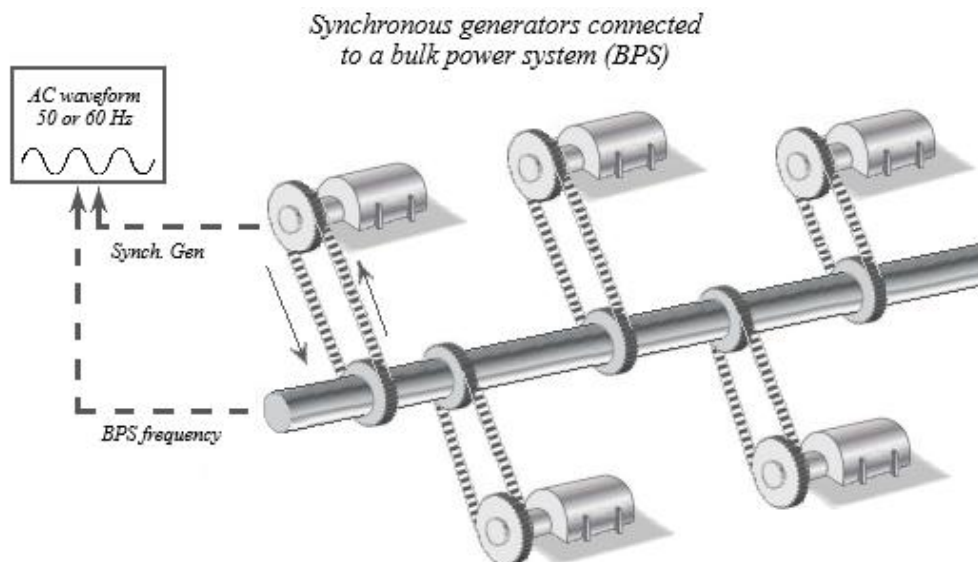


Figure 2.2: A bulk power system containing synchronous generators synchronized at the same frequency due to electromagnetic forces, represented by chains. Figure adapted from [2]

Frequency is a product of the balancing in between supply and demand. In stable operation of a power system, the supply of power will be equal to the demand of power. At such an equilibrium the frequency will be held constant [1].

However, if a contingency event occurs, e.g., due to the loss of a power plant or the loss of a transmission line, the availability of power on the supply side will drop rapidly and nearly instantaneous. As the demand for electric power has not decreased, the same level of electric power will be extracted from the bulk power system [2].

When such a contingency event occurs, the services of inertia have a major stabilizing effect. As stored kinetic energy is extracted from the remaining synchronous generators that has not been tripped or disconnected from the bulk power system, this will compensate for the loss of one or more generators [2]. This service cannot be sustained for more than a few seconds as it will slow down the connected generators, but it will give enough time for other ancillary services to respond and stabilize the frequency [2].

The impact and consequences of a contingency event will depend on several factors. A larger interconnected bulk power system with a substantial number of synchronous generators will have better capabilities to handle a contingency event where one or a few synchronous generators are disconnected from the bulk power system [2]. If a larger synchronous generator is disconnected from a smaller and more isolated grid, due to a contingency event, this will result in a steeper frequency decline, as the contingency size will be much larger with respect to the availability of power and the amount of inertia in the grid [2].

The amount of inertia in a bulk power system, do both scale with the number of connected synchronous generators and the generator size, as a larger synchronous generator will have more mass and furthermore more rotating mass [2]. In addition, it will scale with the type of synchronous generator, as different synchronous generators may have different mass, different shape, and different distribution of the rotating mass [2]. It is feasible to calculate the decline in frequency, by calculating how much each synchronous generator will slow down, as the relationship between rotational speed and energy is known [2].

The services from inertia have typically a timeframe for about 0 to 12 seconds [1].

2.1.3 Primary Frequency Response (PFR) and Secondary Control

The Primary Control functionality is often referred to as Primary Frequency Response (PFR) [1]. PFR is an autonomous service that detects frequency deviations and automatically, with no actions from the system operator, adjusts the operations of the connected generators in such a manner that the frequency is maintained within a desired range [1, 2].

Traditionally, PFR has been provided by mechanically interacting systems in power plants. An example would be the flyball governor, where the ball is moving inward or outward depending on if the frequency is decreasing or increasing. When the rotational speed of the shaft is decreasing, the ball will move inwards, and a mechanical system will adjust the fuel valve so that the power increase. In the same way will an increase of the shaft speed result in an adjustment of the fuel system, so that the power is reduced [2].

This principle is relevant both for fossil fueled plants (steam plants) and hydroelectric plants, where the water valve will be adjusted accordingly [2].

The governors itself, that historically was containing mechanical components, has in many cases been replaced with electronic sensors that measure the frequency and trigger actions in an efficient manner [1, 2]. On the other side do the power control of synchronous generators still rely on mechanical systems to adjust the supply of power [2]. E.g., mechanical valves to adjust the fuel control or the water flow towards a turbine.

The mentioned mechanical systems will always have some time delay in its operation which limits the response rate [2]. Due to this delayed response, inertia has been an important grid service to slow down the rate at which frequency drops and further to avoid under-frequency load-shedding UFLS before the PFR system have had time to complete its task [2].

The services from PFR have typically a timeframe for about 10 to 60 seconds [1].

Figure 2.3, inspired by several figures and explanations in [2], is showing an example of a contingency event, followed by the services of inertia and PFR. It can be observed that the contribution of inertia is slowing the rate of frequency decline and that the PFR is restoring the frequency balance [2].

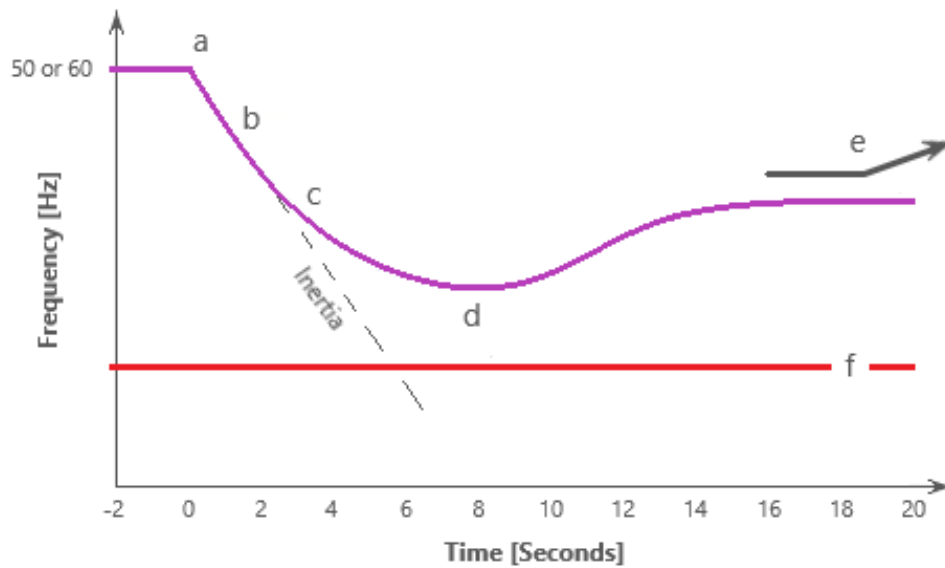


Figure 2.3: Recovery from a contingency event where both inertia and PFR contributed to the recovery

At the left side of figure 2.3, a stable grid operation is shown until a contingency event occurs at point (a) and a starting point for the frequency decline can be observed [2].

It is observed that the frequency decline is slowed by inertia at point (b). This inertial response will slow the remaining connected synchronous generators, as their kinetic rotational energy is converted into real power [2]. As this process is slowing down the connected generators, the frequency will decrease, but at a rate and within a timeframe which make it possible for PFR to respond [2].

At point (c) it is observed that the PFR is start working and that the frequency decline is slowed more than the contribution from inertia alone [2].

And at point (d) it is observed that the PFR is restoring the balance between supply and demand and that the frequency begins to increase. Furthermore, that UFLS is avoided, as the frequency is stabilized, partly restored, and never touched the red line at point (f) [2].

To restore the frequency to a predefined fixed value, i.e., 50 Hz or 60 Hz, other operational services must take actions. This is most often performed in the subsequent seconds and minutes and is indicated at point (e). It will be sent signals to some power plants to increase their power, so that the defined frequency will be achieved [2].

Secondary control functionalities do traditionally provide services at the minute level with a timeframe in between 1 and 10 minutes. However, more modern solutions for secondary control, may have the capability to be much quicker [1].

The secondary control is the type of service that act at point (e) in figure 2.3, to restore the frequency to nominal values.

The secondary control covers a broad spectrum of services, as the secondary control have services deployed to mitigate disturbances and services that has manual inputs through supervisory control and data acquisition (SCADA) systems [1].

Both operating reserves, spinning and supplemental reserves make up and provides services of secondary control functionalities [1].

The spinning reserve is by definition the available additional capacity of base generators synchronized and connected to the power system, well prepared to support the restoration after a contingency event [1, 3].

The spinning reserve is under normal circumstances considered to have a capacity of 15 to 20% of the base load [3].

2.1.4 Renewable Energy Sources (RES)

Power system stability has until today mainly been based on synchronous generators and the control strategies for these generators, that has been developed along with the expansion of the electric grid and that has resulted in decades of experience [4]. These traditional services were reviewed and described in chapter 2.1.1 to 2.1.3.

As Renewable Energy Sources (RES) are being developed and connected to the electric grid, this will result in a larger amount of generation from more nontraditional power sources [4]. This includes sources like solar energy, wind energy and battery storage devices [4]. The increasing amount of IBR's due to RES-integration, will cause a displacement of traditional synchronous generators and their grid stabilizing services [5].

A common denominator for the mentioned RES's, are that they do not have a spinning synchronous generator [4]. Instead, they have power electronic components and are categorized as Inverter-Based Resources (IBR's) [4, 5].

This IBR-based RES-integration implies major challenges with regards to power system stability, as the future interconnected bulk power systems must withstand a situation where both the traditional control responses and properties of synchronous generators are working together with a larger number of IBR's [4].

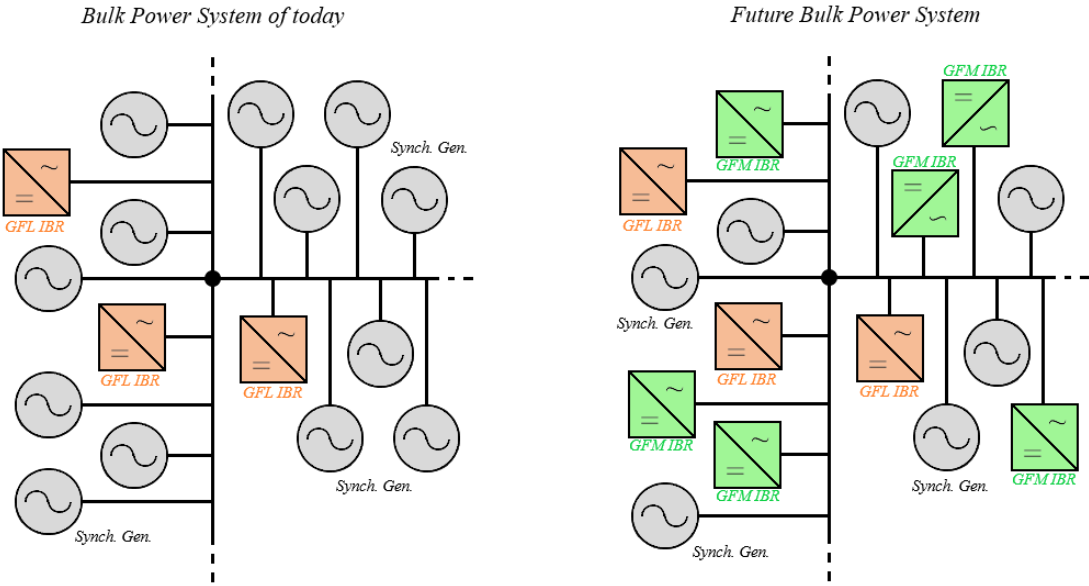


Figure 2.4: Bulk Power System of today and in the future, with a higher RES penetration

2.1.5 Inverter-Based Resources (IBR's)

Inverter-Based Resources (IBR's) are inverters consisting of power electronic components, which normally consist of an AC-side and a DC-side and where the DC-side may be connected directly to a DC-source or through additional DC-DC converters [4].

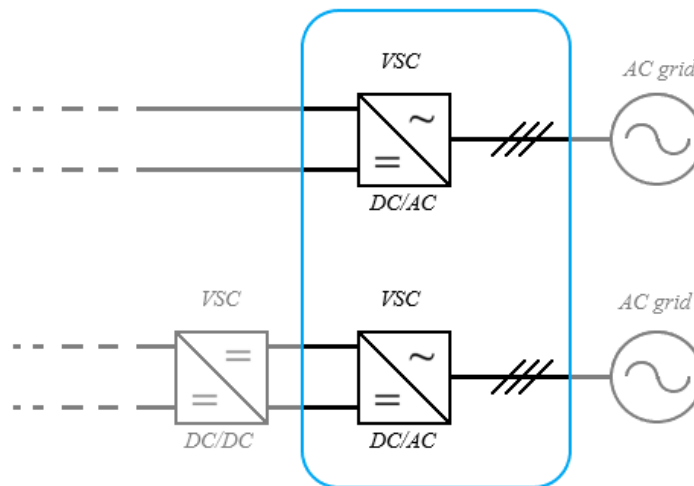


Figure 2.5: Illustration of Inverter-Based Resources (IBR's)

IBR's are divided into two main categories, with regards to their control strategies and their capabilities. These two categories are Grid-Following (GFL) and Grid-Forming (GFM) [4, 5].

Most of today's existing IBR's are GFL and furthermore dependent of being connected to an external AC grid to be able to control their active and reactive current outputs [5].

Some properties and features are unique for GFL inverters, some properties and features are unique for GFM inverters, and some are available for all inverter types [4, 5]. The following properties and features are available for both GFL and GFM inverters [6]:

- IBR's can provide Fast Frequency Response (FFR)
- IBR's can provide Primary Frequency Response (PFR)
- IBR's can provide closed-loop voltage control
- IBR's can provide automatic generation control and dispatchability
- IBR's can provide stability services

The following properties, features, and limitations are applicable for GFL IBR's [6, 7]:

- GFL IBR's assumes that the grid is already formed under normal operations
- GFL IBR's requires Phase-Locked Loop (PLL)
- GFL IBR's have decoupled control of P and Q
- GFL IBR's have a direct-quadrature (dq) vector control of current injected into the grid
- GFL IBR's requires voltage at the point of common coupling (PCC) to supply P and Q
- GFL IBR's cannot operate in a grid with 100 % power electronics penetration, as instability thresholds exists (tipping points)
- GFL IBR's will require a minimum grid strength to establish grid voltage waveform
- GFL IBR's do not have black-start capabilities

The following properties, features are applicable for GFM IBR's [6, 7]:

- GFM IBR's assume they have the responsibility to form and maintain a healthy grid
- GFM IBR's have the capability to control voltage magnitude and frequency/phase
- GFM IBR's have controlled internal voltage phasors
- GFM IBR's have a slight coupling in between P and Q
- GFM IBR's may use PLL control to switch in between different modes
- GFM IBR's have capabilities with regards to voltage persistence and virtual inertia
- GFM IBR's can theoretically operate in a grid with 100 % power electronics penetration. I.e., GFM IBR's can coexist with GFL IBR's
- GFM IBR's are not standardized, and the operational experience is inadequate at a systems perspective
- GFM IBR's can black-start a power system and sustain an islanded operation (islanded grid)

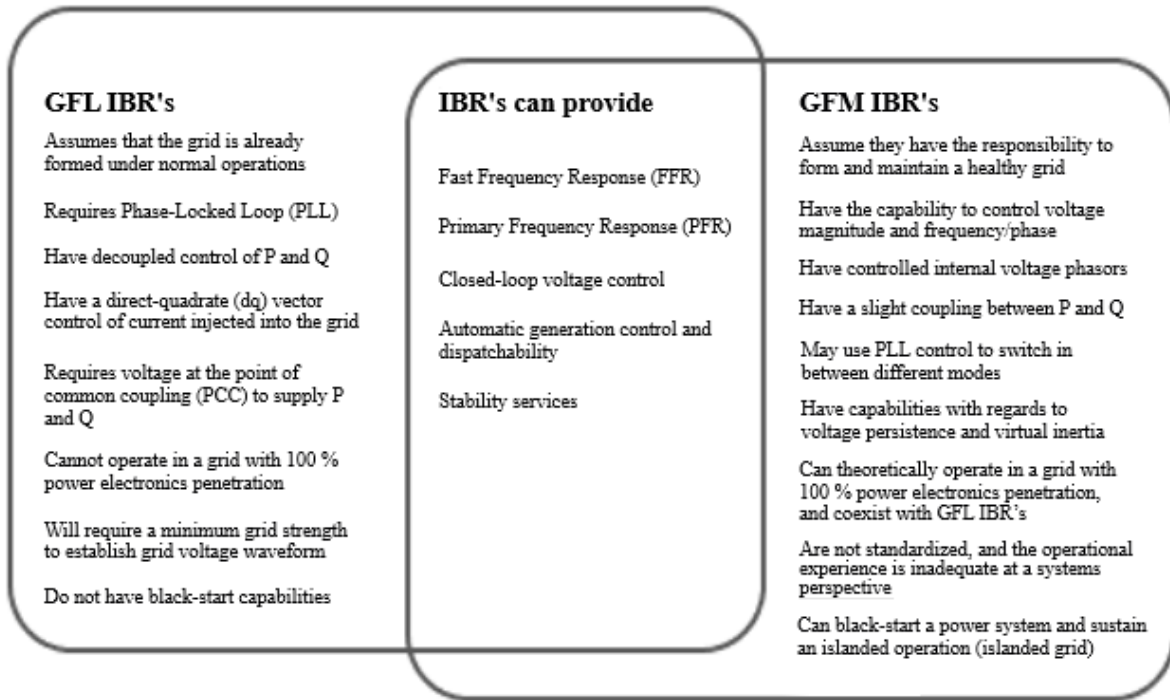


Figure 2.6: The properties of IBR's, GFL IBR's and GFM IBR's put into a figure for comparison

An IBR is built solely with switching devices and will therefore rely on closed-loop controllers. Furthermore, for modern IBR's these closed-loop controllers exist as digital controllers, which are fully programmable and quite flexible [4]. This algorithmic flexibility creates a possibility to develop and evolve the control system in an easily manner [4].

The GFM control strategies can be divided into three subcategories, which will be droop control, virtual synchronous machines (VSM's) / virtual inertia, and virtual oscillator controllers [4]. Both HVDC systems and battery systems are candidates for grid forming inverter operations, i.e., candidates for being GFM IBR's [8].

2.1.6 Fast Frequency Response (FFR)

Fast Frequency Response (FFR) is a term used for resources that has the capability to increase their net supply of energy in a fast manner and much faster than traditionally PFR relying on mechanical systems [2]. One type of resources that can provide FFR, are the mentioned IBR's. This applies to both GFM IBR's and GFL IBR's [2, 6].

FFR is one type of service that will help mitigate the declining inertia in the bulk power system, due to the RES-integration and a corresponding increasing percentage of IBR's in the grid. With regards to the decline of inertia, the FFR will cause a counterbalancing effect as the rapid frequency decline due to the lack of inertia, will be compensated by a quicker response from FFR [2]. I.e., a more rapid injection of active power into the grid than traditional PFR.

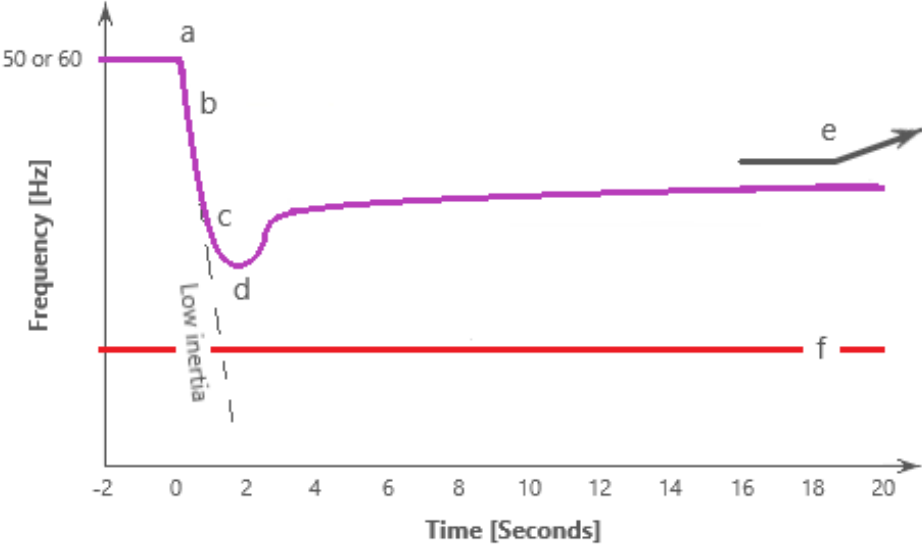


Figure 2.7: Recovery from a contingency event where both low inertia and FFR contributed to the recovery

In figure 2.7 the services from FFR are visual depicted. This figure is adapted from figure 2.3 in chapter 2.1.3. Except for the amount of inertia and the FFR, the initial grid conditions and the contingency size can be assumed to be equal. By comparison of figure 2.3 and figure 2.7, it can be observed that UFLS at line (f) would have been reached, if it was not for the quick response of FFR at point (c) and (d), due to the steep frequency decline at point (b) as a direct consequence of low inertia.

2.1.7 Grid-Forming (GFM) Control Strategies

As mentioned in chapter 2.1.5, GFM control strategies can be divided into three subcategories, which will be droop control, virtual synchronous machines (VSM's) / virtual inertia, and virtual oscillator controllers [4].

Whereas GFL IBR's will behave as current sources, GFM IBR's will behave as voltage sources, which complies with the droop laws [4]. This is illustrated in figure 2.8 for GFL IBR's and in figure 2.9 for GFM IBR's.

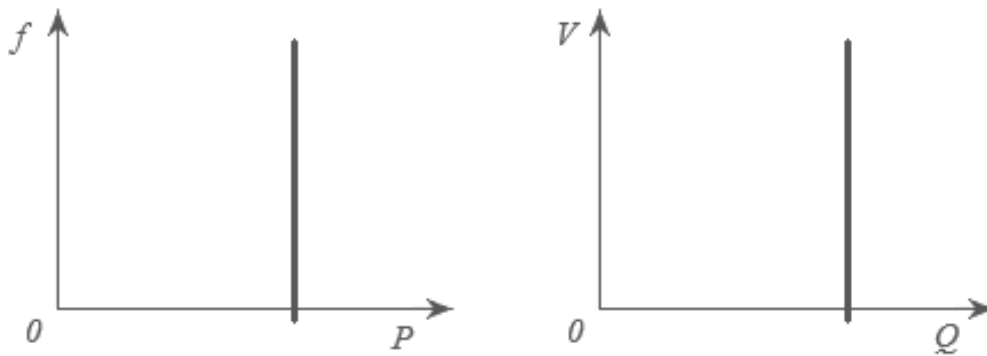


Figure 2.8: Illustration of the $P - f$ ($P - \omega$) and $Q - V$ relationships for GFL IBR's

The droop control was first proposed early in the 1990's and is considered to be the most well-established GFM control [4]. The droop laws are well known for its linear trade-off between frequency and voltage versus real power and reactive power and are described as a relationship between $P - \omega$ (real power – frequency) and $Q - V$ (reactive power – voltage) [4].

The droop laws have some characteristic properties that applies both for traditional synchronous machines and IBR's. I.e., they enable the possibility to reach the same frequency for all units and furthermore achieve a system-wide synchronization. Furthermore, they enable the possibility for power sharing where each connected unit supplies power in direct proportion to the capacity of the respective unit, or according to the programmable droop slope for the unit [4].

Another GFM control strategy is the Virtual Synchronous Machine (VSM) or virtual inertia. The complexity of this control strategy can vary majorly. In one end of the spectrum the synchronverters can be found, which are detailed electromechanical models that to a substantial extent match the real machine characteristics, contains virtual flux dynamics, and that contains both $P - \omega$ and $Q - V$ characteristics for synchronous machines [4]. On the other side of the mentioned spectrum, the virtual inertia can be found, which only emulates the dynamic of a rotor and the corresponding steady-state $P - \omega$ droop of this rotor [4].

The third GFM control strategy to be mentioned in this thesis, is the virtual oscillator controller. This controller is based on the emulation of nonlinear oscillators and has emerged in the latest years [4]. This type of control strategy does share some common denominators with the VSM, as a digital model is processing real-time measurements and have output variables that modulate the power stage of the inverter [4]. Except for this, the model will in this case behave as an oscillator circuit, with a natural frequency. This frequency will coincide with the connected grid frequency and parameters must be tuned to be able to change the nominal voltage and to be able to control the bandwidth [4].

Regardless of the GFM control strategy, i.e., droop control, VSM/inertia or virtual oscillators, the output terminals will behave as a voltage source which enables the droop laws, illustrated in figure 2.9.

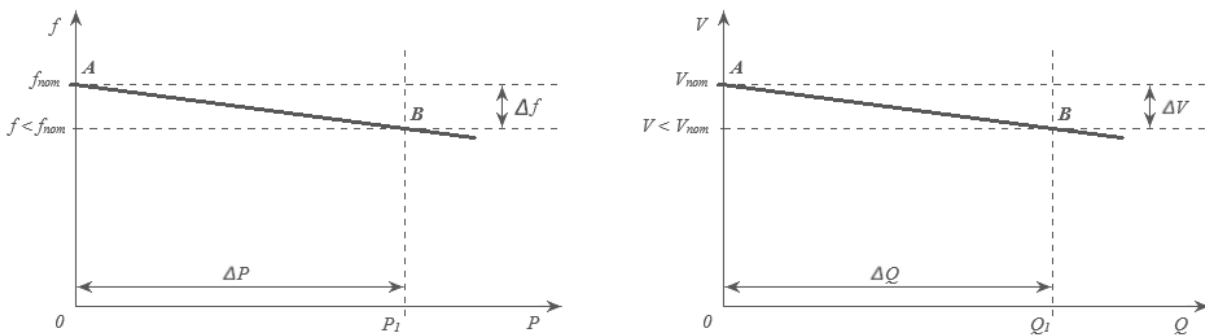


Figure 2.9: Illustration of the $P - f$ ($P - \omega$) and $Q - V$ relationships for GFM IBR's

2.1.8 Geographical Considerations

RES integration and an increasing amount of IBR's in the bulk power system, comes with some considerations. Control functionalities for IBR's to ensure power system stability, interoperability, and coordination, becomes very advanced and complicated [5].

Instability concerns are especially applicable for power systems with a low system strength and a high level of GFL IBR's, as the voltage is sensitive to current injections, due to the technical nature of GFL IBR's. As the operation of GFL IBR's closely rely on measurements, a deviation, or an inaccuracy in the measurement, will lead to an incorrect behavior of the GFL IBR control, which further may cause power system instability [5].

The utilization of GFM controlled IBR's for battery solutions has recently been identified to have a strong stabilizing influence [5]. Non-mandatory GFM power source specifications are being developed in Great Britain and in Australia it is being performed studies to identify to which extent GFM IBR's can provide enough system strength to support GFL IBR's [5].

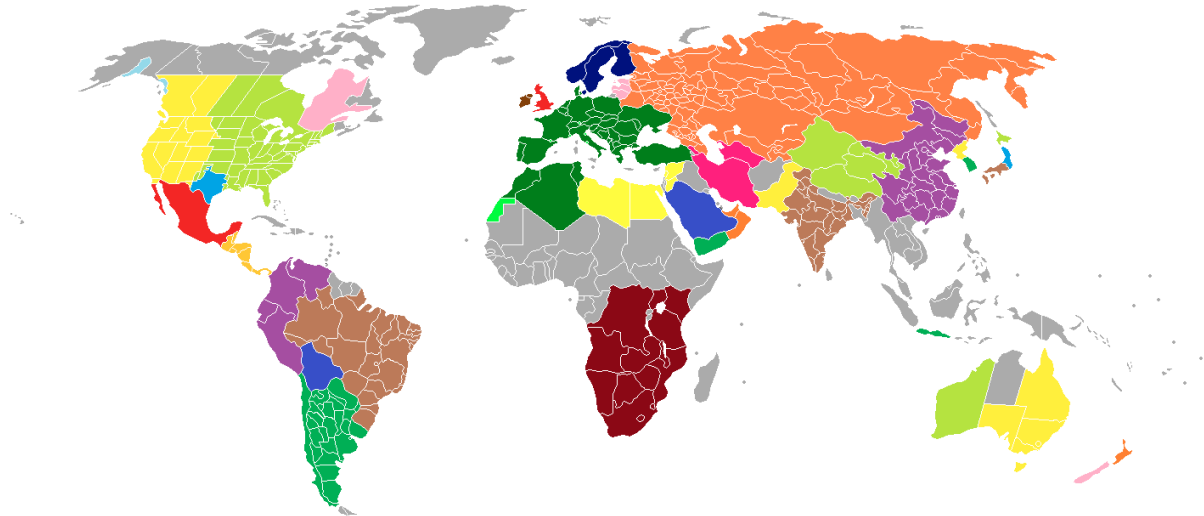


Figure 2.10: Wide area synchronous grid. Source: Wikimedia Commons [9]

Supported by GFM controls and energy storage, some smaller islanded networks are already operating at a nearly 100 % RES IBR penetration [4]. Based on 2018 data, the Ta'u Island, American Samoa have both 100 % instantaneous power and 100 % annual energy from RES IBR's [10]. Also based on 2018 data, the King Island in Australia do have the possibility to have 100 % instantaneous power and 65 % annual energy from RES IBR's, the Maui Island

in Hawaii have the possibility for 76 % instantaneous power and 36 % annual energy from RES IBR's [10]. Furthermore, Ireland has the possibility for 65 % instantaneous power and 29 % annual energy from RES IBR's, according to the 2018 data [10]. But newer data indicates that the instantaneous power has increased to 75 %, if the HVDC links to/from Ireland are included [5]. Larger bulk power systems, like the Western Interconnection in the USA, do only have 24 % instantaneous power and only 10 % of the annual energy from IBR's, based on 2018 data [10].

For the largest bulk power systems, like the Continental Europe (UCTE), the Eastern Interconnection and the Western Interconnection in USA, with power capacity of several hundred GW's, any operation at 100 % IBR penetration is not foreseen the next years to come [5]. However, it is a concern that areas with a high level of RES integration and IBR penetration, will be disconnected from the interconnected bulk power system [5].

An example would be the South Australian power system which is relatively isolated and that may be disconnected from the much larger Australian power system, in case the point of connection experiences overload conditions [11]. The Hornsdale Power Reserve, consisting of lithium-ion batteries with a capacity of 100 MW / 129 MWh, makes up a reserve that has prevented such a disconnection for at least two occasions where a trip of a large coal plant has caused a contingency event [11].

GFM IBR's in large bulk power systems are still premature and many open research questions must be worked on, before the largest bulk power systems are prepared for a significant higher percentage of its power sources covered from IBR's [4].

It is foreseen that the incorporation of GFM controls will be based on experience gained from operations in smaller grids and that the incorporation into bulk power systems will take several years [4]. Furthermore, it is foreseen that GFM controls will be present in microgrids from now and in a ten-year perspective, that instantaneous GFM control challenges in islanded grids will be experienced in the near future, that GFM controls in larger grids will be implemented in a three to fifteen year perspective from now, that instantaneous GFM control challenges will be experienced in weak parts of bulk power systems after three years or more from today, and finally that the incorporation of GFM controls in the large bulk power systems will happen ten to thirty years from today [12].

2.2 Electrochemical Energy Storage Technologies

In this chapter, literature describing relevant electrochemical energy storage technologies are reviewed. An extensive search for literature comparing relevant technologies for grid-scale electrochemical energy storage has been performed. In addition, a thorough literature search has been performed for each individual technology. The content in this chapter is limited to the technologies that seem to be the most relevant for grid-scale energy storage and thus further assessments.

The selected electrochemical energy storage technologies for further assessments will be the following four battery technologies: Lithium-ion, Sodium-sulfur, Flow Batteries and Lead-Acid. Including sub-categories of the lithium-ion technology.

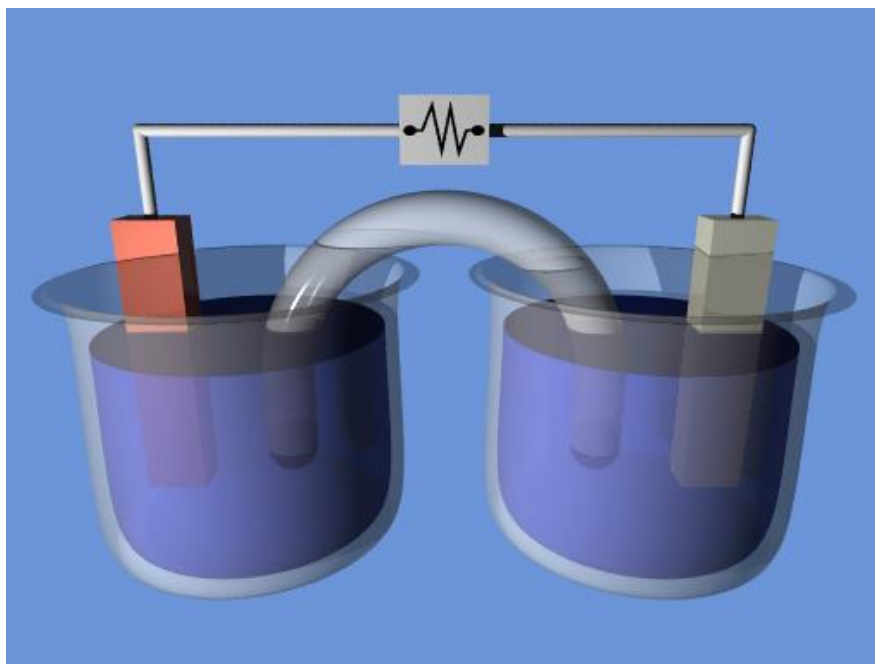


Figure 2.11: Electrochemical cell. Source: Wikimedia Commons [13]

Electrochemical energy storage systems, like rechargeable batteries, store electricity in the form of chemical energy by using a series of reversible chemical reactions [11].

2.2.1 Batteries

The most applied, and the most common form of electrochemical energy storage, are batteries. Batteries have the capability to change the output in the range of sub-seconds to several minutes and may have an operational duration lasting for several hours [11].

The properties of some common battery technologies can be visually observed in the Ragone plot in figure 2.12 [14]. It is tough noted that this figure is an example that may not correlate with the data in the further review and assessments, due to the rapid evolvement of different technologies.

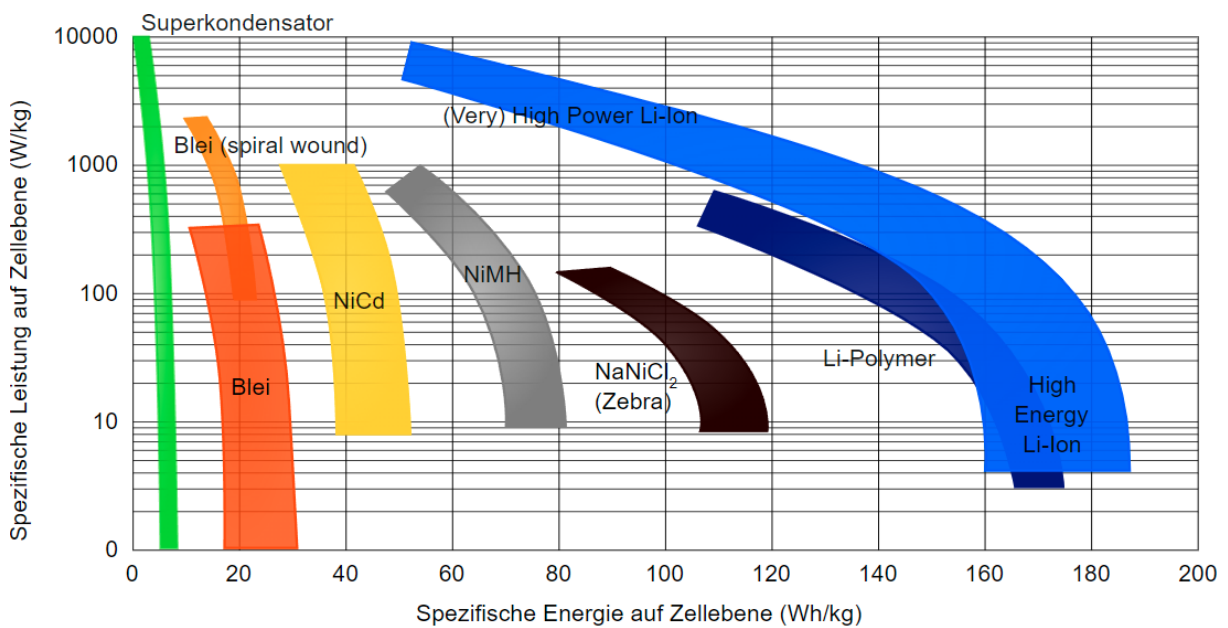


Figure 2.12: Ragone plot showing the properties for some common battery technologies.
Source: Wikimedia Commons [14]

The cost estimation data used in this review corresponds to the cost of the total ESS installation. For more detailed cost data, the reader is encouraged to review report [15].

2.2.2 Lithium-ion

Lithium-ion is widely commercialized and currently the dominating battery technology for new utility-scale electrochemical energy storage facilities [11]. The popularity of this technology is driven by a steep drop in the battery pack prices the last decade, i.e., a decline of 89 % in between 2010 and 2020 [11]. Other contributing factors are well-developed supply chains and robust manufacturing capabilities [11].

Lithium-ion batteries provides the possibility to achieve the same energy and power with both less and lighter batteries, than other competing technologies, as lithium-ion batteries have significantly higher power density compared to other relevant battery technologies [11].

This widely commercialized technology has a cost range between 1'408 to 1'947 USD per kilowatt (\$/kW) and corresponding a cost range between 352 to 487 USD per kilowatt hour (\$/kWh), depending on the size of the battery package and the selected chemistry [11, 16]. The mentioned data corresponds to the estimated 2020 cost for 10 MW / 4-hour NMC [15].

The reaction time is at a sub-second to second level and the duration of discharge at max power capacity is typically minutes to a few hours [11, 16]. Furthermore, the round-trip efficiency is between 86-88 % and the expected lifetime is 10 years [11, 16]. The cycle life is between 1'000 to 2'000 cycles, depending on the selected chemistry, temperatures, the behavior of the storage system and stress due to use cases [11, 17].

As already mentioned, the lithium-ion battery has a very high energy density and a very high power density, compared to its competitors. This energy- and power density will be depending on the selected chemistry, cell design and power electronics configurations [11, 17]. The energy density is considered to be in the area between 210 to 325 Watt hours per kilogram (Wh/kg) and the power density is considered to be in the area between 4'000 to 6'500 Watt per kilogram (W/kg) [11, 17].

The operating temperature for the lithium-ion battery will be between -20 to +65 degrees Celsius ($^{\circ}C$) [11, 17], which is the only assessed battery technology that has an operating temperature below zero degrees Celsius.

The lithium-ion battery technology is increasingly used for stationary utility-scale energy storage applications [11]. Furthermore, this battery technology is used for ancillary services

like frequency response, to ensure a stable balance between supply and demand at short timescales [11]. The properties of the lithium-ion battery with regards to long cycle life and quick response time resulting in that this battery technology is a good candidate for such services that requires deep and frequent cycling [11].

Thermal runaway is a condition where the temperature inside the battery is becoming high enough to trigger a self-sustaining heat generation [11]. Furthermore, this condition will easily lead to battery failures or fires [11]. As lithium tends to have a low runaway temperature, fire suppression systems and thermal management are important factors to consider in the design of a lithium-ion battery facility [11]. These mitigations may increase the overall costs [11].



*Figure 2.13: LFP cells connected in parallel and series.
Source: Wikimedia Commons [18]*

The lithium-ion battery technology consists of sub-categories, using different chemistries and configurations, leading to slightly different operating parameters [11].

Lithium Nickel Manganese Cobalt (NMC) is by far the most used chemistry as of today [11]. NMC is competing with the chemistries Lithium Nickel Cobalt Aluminum (NCA) and Lithium Iron Phosphate (LFP), where both NCA and specially LFP will take over most of the market share from NMC during the next decades [11].

NMC have an energy density of 325 watt-hours per liter (Wh/L), a power density of 6'500 watt per liter (W/L), an operating temperature between -20 to +55 degrees Celsius (°C), a cycle life around 1'200 cycles and a self-discharge equal to 1 % per month [11, 19].

Furthermore, an ESS installation consisting of 100 MW / 4-hours NMC batteries, is estimated to have an average cost of 1'581 \$/kW and a cost range between 1'320 and 1'827 \$/kW in 2020 [15]. In 2030 the cost range is predicted to be between 965 and 1'279 \$/kW and with an assumed average cost of 1'128 \$/kW, for a 100 MW / 4-hour plant [15].

NCA have an energy density between 210 to 600 watt-hours per liter (Wh/L), a power density between 4'000 to 5'000 watt per liter (W/L), an operating temperature between -20 to +60 degrees Celsius (°C), a cycle life greater than 1'000 cycles and a self-discharge rate between 2 to 10 % per month [11, 19].

LFP have an energy density between 220 to 250 watt-hours per liter (Wh/L), a power density equal to 4'500 watt per liter (W/L), an operating temperature between -20 to +60 degrees Celsius (°C), a cycle life around 2'000 cycles and a self-discharge lower than 1 % per month [11, 19]. Furthermore, an ESS installation consisting of 100 MW / 4-hours LFP batteries, is estimated to have an average cost of 1'541 \$/kW and a cost range between 1'302 and 1'752 \$/kW in 2020 [15]. In 2030 the cost range is predicted to be between 944 and 1'249 \$/kW and with an assumed average cost of 1'081 \$/kW, for a 100 MW / 4-hour plant [15].

*Table 2.1:
Summary of reviewed data for lithium-ion batteries*

Battery technology	Cost range in USD per power unit (\$/kW)		Cost range in USD per energy unit (\$/kWh)		Commercial availability	Reaction time	Duration of discharge at max power capacity	Power density		Energy density		Round-trip efficiency	Operating temperature	Rate of self-discharge	Cycle life (# of cycles)	Expected lifetime	Foreseen usage next decades
	Low	High	Low	High				Low	High	Low	High						
Lithium-ion in general	1'302	1'947	352	487	Widely	Sub-seconds to seconds	Minutes to a few hours	4'000 W/kg	6'500 W/kg	210 Wh/kg	325 Wh/kg	86 to 88 %	-20 to +65 °C		1'000 to 2'000	10 years	Increasing
NMC	1'320	1'827			Widely			6'500 W/L		325 Wh/L			-20 to +55 °C	1% per month	around 1'200		Declining compared to NCA/LFP
NCA					Widely			4'000 W/L	5'000 W/L	210 Wh/L	600 Wh/L		-20 to +60 °C	2 to 10 % per month	above 1'000		Increasing
LFP	1'302	1'752			Widely			4'500 W/L		220 Wh/L	250 Wh/L		-20 to +60 °C	1% per month	around 2'000		Increasing

Utility-scale lithium-ion battery energy storage has been heavily deployed during the last years. A reference project is the Hornsdale Power Reserve in South Australia [11, 20]. This BESS plant consists of a 100 MW / 129 MWh lithium-ion battery that was completed in 2017 [11, 20]. In September 2020, this plant was expanded with a 50 MW / 64,5 MWh battery, so that the total power capacity reached 150 MW [20].

Another reference project is the Victorian Big Battery, which is a 300 MW / 450 MWh grid-scale BESS project in Geelong, Australia, that was put in operation December 8, 2021 [21]. The plant consisting of 210 BESS units is covering an area smaller than a football oval, due to the high power and energy density of the lithium-ion battery [21].

Future research, technology development and improvements in lithium-ion battery technologies will mainly be focused on increasing the energy density and the power output, furthermore, to increase the safety of the batteries, to reduce the overall cost, and maybe the most important task – to reduce the reliance on scarce minerals [11].

Some novel technologies are already being assessed. The lithium-air battery, which both can reduce the reliance on scarce minerals, be more cost efficient and achieve a higher energy density [11]. Another technology is the solid-state lithium-ion battery, which have improved energy density and lesser safety concerns, as this battery chemistry is using solid electrolytes [11].

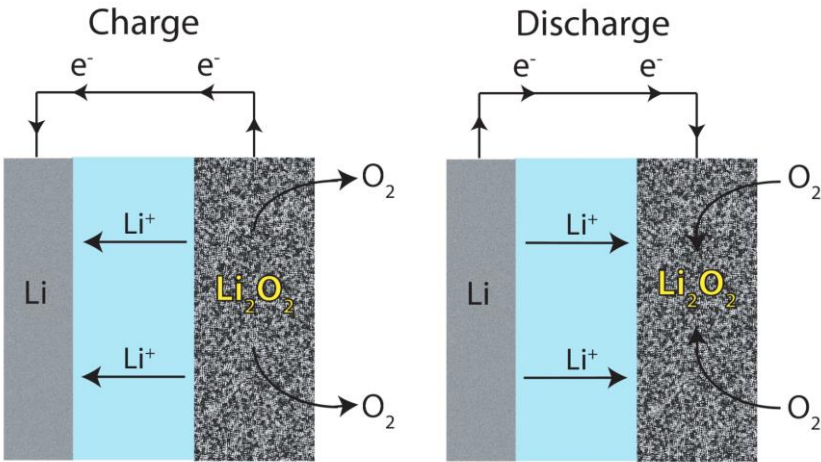


Figure 2.14: Charge-discharge diagram for a lithium-air battery.
 Source: Wikimedia Commons [22]

The lithium-ion battery review can be summed-up with a quotation from the very thorough report *USAID GRID-SCALE ENERGY STORAGE TECHNOLOGIES PRIMER* [11], used as one of the main sources for data in the review performed in this chapter of the thesis:

“Lithium-ion is a mature energy storage technology with established global manufacturing capacity driven in part by its use in electric vehicle applications. The overlap between the transportation and power system sectors have enabled steep price declines in technology costs for lithium-ion batteries, driving higher deployments. In utility-scale power sector applications, lithium-ion has been used predominantly for short-duration, high-cycling services such as frequency regulation, although it is increasingly used to provide peaking capacity and energy arbitrage services in certain jurisdictions. Lithium-ion has a typical duration in the 2- to 4-hour range, with price competitiveness decreasing at longer durations. One major technical issue with lithium-ion is fire safety, as the chemistry can suffer thermal runaway leading to fire concerns. Recent battery pack technology and software innovations are addressing safety concerns related to thermal runaway” [11].

2.2.3 Sodium-sulfur

Sodium-sulfur batteries work in principle by a reversible redox reaction, between molten sodium (Na) and sulfur (S), to electrically charge and discharge [11]. This battery technology is considered to be a high-temperature battery, as it is operating at temperatures around 300 degrees Celsius to utilize a solid electrolyte to manage reactions between liquid electrodes [11].

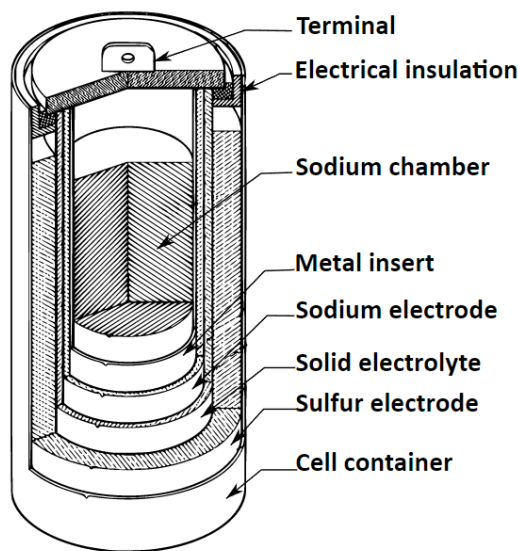


Figure 2.15: Sodium-sulfur battery. Source: Wikimedia Commons [23]

The sodium-sulfur battery has a very rapid response time, estimated to be around 1 millisecond, in addition it has a high reliability, high maintainability, a high energy density and a low self-discharge [11, 24].

This initial commercialized technology had in 2018 a cost range between 2'394 to 5'170 USD per kilowatt (\$/kW) and corresponding a cost range between 599 to 1'293 USD per kilowatt hour (\$/kWh) [11, 16].

The reaction time is at a sub-second level and the duration of discharge at max power capacity is typically several hours [11, 16]. Furthermore, the round-trip efficiency is between 77-83 % and the expected lifetime is 15 years [11, 16]. The cycle life is equal to around 4'500 cycles, depending on environmental temperatures, the behavior of the storage system and stress due to use cases [11, 17].

As for the lithium-ion battery, the sodium-sulfur battery has a very high energy density, but the power density is significantly lower for the sodium-sulfur battery compared with the lithium-ion case [11]. The energy density is considered to be in the area between 150 to 240 Watt-hours per kilogram (Wh/kg) and the power density is considered to be in the area between 120 to 160 Watt per kilogram (W/kg) [11, 17].

The operating temperature for the sodium-sulfur battery is between 300 to 350 degrees Celsius (°C) [11, 17], which makes sodium-sulfur the reviewed battery technology with the highest operating temperature.

Table 2.2:
Summary of reviewed data for sodium-sulfur batteries

Battery technology	Cost range in USD per power unit (\$/kW)		Cost range in USD per energy unit (\$/kWh)		Commercial availability	Reaction time	Duration of discharge at max power capacity	Power density		Energy density		Round-trip efficiency	Operating temperature	Rate of self-discharge	Cycle life (# of cycles)	Expected lifetime	Foreseen usage next decades
	Low	High	Low	High				Low	High	Low	High						
Sodium-sulfur	2'394	5'170	599	1'293	Initial	Sub-seconds	Several hours	120 W/kg	160 W/kg	150 Wh/kg	240 Wh/kg	77 to 83 %	300 to 350 °C	Very low	around 4500	15 years	Increasing for long duration services

As sodium-sulfur batteries typically have a long discharge time at maximum power output level, i.e., around 6 to 8 hours, has a high energy density, but a significant lower power density than for the lithium-ion technology, this makes sodium-sulfur a good candidate for long duration services [11].

In 2018 it was commissioned around 190 MW sodium-sulfur batteries around the world [11]. It has been deployed test projects with hybrid solutions where the sodium-sulfur is designed for the long duration services and the lithium-ion is designed to handle the short-term fluctuations [11].

Future research, technology development and improvements in sodium-sulfur battery technologies will mainly be focused on reducing the high operating temperature, furthermore, to reduce the internal battery corrosion, that may lead to higher losses with regards to self-discharge [11]. A more advanced sodium-sulfur technology can be operated between 100 to 200 degrees Celsius, in addition to this have researchers lately developed nanomaterials that will contribute to a higher performance for room-temperature sodium-sulfur batteries [11].

The sodium-sulfur battery review can be summed-up with a quotation from the very thorough report *USAID GRID-SCALE ENERGY STORAGE TECHNOLOGIES PRIMER* [11], used as one of the main sources for data in the review performed in this chapter of the thesis:

“Sodium-sulfur is an energy storage technology in the initial commercialization phase, marked by high energy density, low levels of self-discharge (which correspond to higher efficiencies), and relatively long cycle life. These storage systems rely on common, abundant, and cheap materials, which may help drive down costs relative to storage systems reliant on scarce minerals. Despite these advantages, sodium-sulfur has seen relatively little deployment due to its high operating temperature requirements (300°–350°C). Given its long duration capability, on the scale of several hours, and its high cycle life, sodium-sulfur may be well suited for longer duration services such as peaking capacity and energy arbitrage” [11].

2.2.4 Flow batteries

The flow battery has an electrolyte solved in liquid and that are stored in tanks [11, 15]. This electrolyte liquid is pumped through a membrane and as the electrolyte liquid is separated from the reactive electrodes, this technical solution is considered to be safe compared to other battery technologies [11].

The power and energy levels are also independently scalable, as the power capacity is closely tied to the surface area of the electrodes, and as the energy capacity is closely tied to the physical capacity of the connected storage tanks, i.e., the size of the reservoir [11].

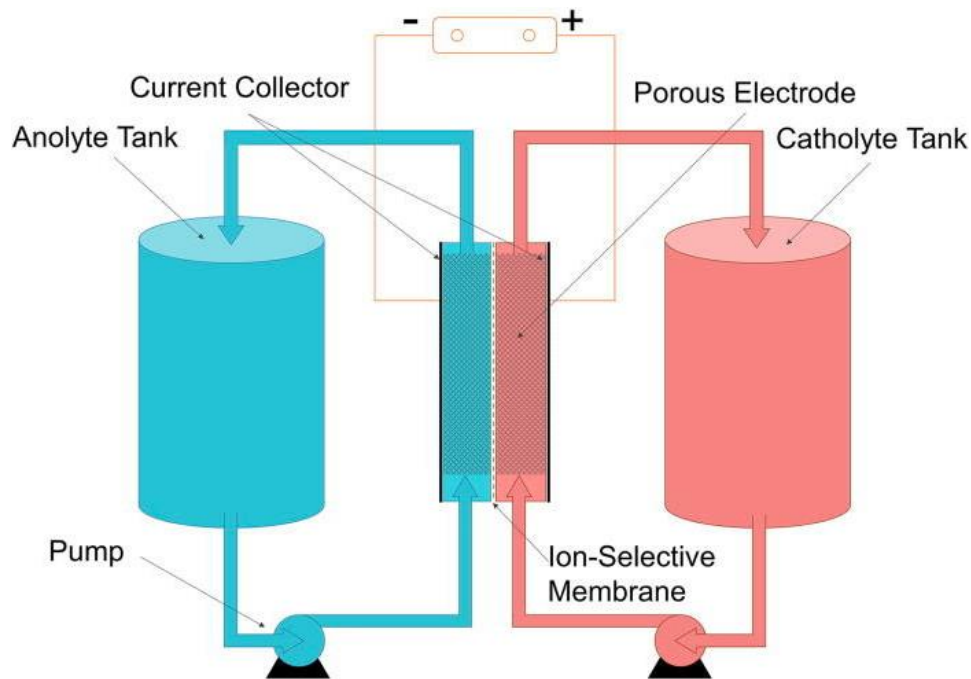


Figure 2.16: Redox Flow Battery. Source: Wikimedia Commons [25]

This initial commercialized technology had in 2020 a cost range between 1'995 to 2'438 USD per kilowatt (\$/kW) and corresponding a cost range between 499 to 609 USD per kilowatt hour (\$/kWh) [11, 16]. This corresponds to the estimated 2020 cost for a 10 MW / 4-hours Vanadium Redox Flow battery [15].

The estimated 2020 average cost for a 100 MW / 4-hour Vanadium Redox Flow ESS is 2'070 \$/kW and with a cost range between 1'863 to 2'277 \$/kW [15]. The predicted average cost for 2030 is 1'656 \$/kW and with a cost range between 1'388 to 1'864 \$/kW [15].

The reaction time is at a sub-second to seconds level and the duration of discharge at max power capacity is typically several hours [11, 16]. Furthermore, the round-trip efficiency is between 65-70 % and the expected lifetime is 15 years [11, 16]. The cycle life is in the area between 12'000 to 14'000 cycles, depending on environmental temperatures, the behavior of the storage system and stress due to use cases [11, 17].

Compared to the lithium-ion battery and the sodium-sulfur battery, the flow battery has a very low energy density and a very low power density [11, 17]. The energy density is considered to be in the area between 10 to 50 Watt-hours per kilogram (Wh/kg) and the power density is considered to be in the area between 0.5 to 2 Watt per kilogram (W/kg) [11, 17].

The operating temperature for the flow battery is between 5 to 45 degrees Celsius (°C) [11, 17].

*Table 2.3:
Summary of reviewed data for flow batteries*

Battery technology	Cost range in USD per power unit (\$/kW)		Cost range in USD per energy unit (\$/kWh)		Commercial availability	Reaction time	Duration of discharge at max power capacity	Power density		Energy density		Round-trip efficiency	Operating temperature	Rate of self-discharge	Cycle life (# of cycles)	Expected lifetime	Foreseen usage next decades
	Low	High	Low	High				Low	High	Low	High						
Flow batteries	1'863	2'438	499	609	Initial	Sub-seconds to seconds	Several hours	0.5 W/kg	2 W/kg	10 Wh/kg	50 Wh/kg	65 to 70 %	5 to 45 °C		12'000 to 14'000	15 years	Increasing for long duration services



Figure 2.17: 1 MW 4 MWh Containerized vanadium flow battery. Source: Wikimedia Commons [26]

The flow battery review can be summed-up with a quotation from the very thorough report *USAID GRID-SCALE ENERGY STORAGE TECHNOLOGIES PRIMER* [11], used as one of the main sources for data in the review performed in this chapter of the thesis:

“Flow batteries are in the initial stages of commercialization. The technology is marked by long durations, the ability to deeply discharge its stored energy without damaging the storage system, and exceedingly long life cycles. Flow batteries may be uniquely situated for longer duration services such as load following or peaking capacity. While flow batteries have higher upfront costs than lithium-ion, their longer life cycle can lead to significantly lower lifetime costs. Flow batteries are also typically safer and are less reliant on rare materials, depending on the specific chemistry. Given flow batteries’ low energy and power density, these systems tend to be larger than other equivalent storage technologies” [11].

2.2.5 Lead-Acid

The lead-acid battery technology is for most people well-known as it has been on the market for decades and has commonly been used as a start-battery for fossil fueled vehicles.



Figure 2.18: A traditional lead-acid car battery. Source: Wikimedia Commons [27]

This widely commercialized technology had in 2020 a cost range between 1'520 to 1'792 USD per kilowatt (\$/kW) and corresponding a cost range between 380 to 448 USD per kilowatt hour (\$/kWh) [11, 16]. This corresponds to the estimated 2020 cost for a 10 MW / 4-hours Lead-acid ESS [15].

The estimated 2020 average cost for a 100 MW / 4-hour Lead-acid ESS is 1'544 \$/kW and with a cost range between 1'419 to 1'672 \$/kW [15]. The predicted average cost for 2030 is 1'322 \$/kW and with a cost range between 1'211 to 1'436 \$/kW [15].

The reaction time is at level of seconds and the duration of discharge at max power capacity is typically minutes to a few hours [11, 16]. Furthermore, the round-trip efficiency is between 79-85 % and the expected lifetime is 12 years [11, 16].

The cycle life is in the area between 500 to 1000 cycles, depending on environmental temperatures, the behavior of the storage system and stress due to use cases [11, 17].

Compared to the lithium-ion battery and the sodium-sulfur battery, the lead-acid battery has a very low energy density and a very low power density [11, 17]. The energy density is considered to be in the area between 30 to 50 Watt-hours per kilogram (Wh/kg) and the power density is considered to be in the area between 30 to 50 Watt per kilogram (W/kg) [11, 17].

The operating temperature for the lead-acid battery is between 18 to 45 degrees Celsius (°C) [11, 17].

Table 2.4:
Summary of reviewed data for lead-acid batteries

Battery technology	Cost range in USD per power unit (\$/kW)		Cost range in USD per energy unit (\$/kWh)		Commercial availability	Reaction time	Duration of discharge at max power capacity	Power density		Energy density		Round-trip efficiency	Operating temperature	Rate of self-discharge	Cycle life (# of cycles)	Expected lifetime	Foreseen usage next decades
	Low	High	Low	High				Low	High	Low	High						
Lead-acid	1'419	1'792	380	448	Widely	Seconds	Minutes to a few hours	30 W/kg	50 W/kg	30 Wh/kg	50 Wh/kg	79 to 85 %	18 to 45 °C		500 to 1'000	12 years	Off-grid applications

The lead-acid battery review can be summed-up with a quotation from the very thorough report *USAID GRID-SCALE ENERGY STORAGE TECHNOLOGIES PRIMER* [11], used as one of the main sources for data in the review performed in this chapter of the thesis:

“Lead-acid energy storage is a mature, widely commercialized technology driven by its applications in transportation. Lead-acid is marked by low upfront costs relative to newer technologies, including lithium-ion; however, several characteristics, such as its short cycle life and its inability to remain uncharged for long periods or to be deeply discharged without permanent damage, have limited its applications in utility-scale power system applications. Ancillary services that require frequent, shallow charging and discharging like frequency regulation may be better suited for lead-acid, compared to less frequent, deeper discharge applications like peak demand reduction. Despite these limitations, lead-acid is still used in off-grid applications such as in isolated microgrids, particularly where upfront costs can be a barrier” [11].

2.2.6 Summary of the Electrochemical Review

In chapter 2.2.2 to chapter 2.2.5 the selected battery chemistries were reviewed. The key-takeaway from this review is put into table 2.5.

The assessment of the reviewed data is performed in chapter 3.2 where an updated version of table 2.5 is added, providing a visual expression of some of the selected parameters for the decision making.

Table 2.5:

Summary of the review in chapter 2.2, for comparison purpose

Battery technology	Cost range in USD per power unit (\$/kW)		Cost range in USD per energy unit (\$/kWh)		Commercial availability	Reaction time	Duration of discharge at max power capacity	Power density		Energy density		Round-trip efficiency	Operating temperature	Rate of self-discharge	Cycle life (# of cycles)	Expected lifetime	Foreseen usage next decades
	Low	High	Low	High				Low	High	Low	High						
Lithium-ion in general	1'302	1'947	352	487	Widely	Sub-seconds to seconds	Minutes to a few hours	4'000 W/kg	6'500 W/kg	210 Wh/kg	325 Wh/kg	86 to 88 %	-20 to +65 °C		1'000 to 2'000	10 years	Increasing
NMC	1'320	1'827			Widely			6'500 W/L		325 Wh/L			-20 to +55 °C	1% per month	around 1'200		Declining compared to NCA/LFP
NCA					Widely			4'000 W/L	5'000 W/L	210 Wh/L	600 Wh/L		-20 to +60 °C	2 to 10 % per month	above 1'000		Increasing
LFP	1'302	1'752			Widely			4'500 W/L		220 Wh/L	250 Wh/L		-20 to +60 °C	1% per month	around 2'000		Increasing
	Low	High	Low	High				Low	High	Low	High						
Sodium-sulfur	2'394	5'170	599	1'293	Initial	Sub-seconds	Several hours	120 W/kg	160 W/kg	150 Wh/kg	240 Wh/kg	77 to 83 %	300 to 350 °C	Very low	around 4'500	15 years	Long duration services
	Low	High	Low	High				Low	High	Low	High						
Flow batteries	1'863	2'438	499	609	Initial	Sub-seconds to seconds	Several hours	0.5 W/kg	2 W/kg	10 Wh/kg	50 Wh/kg	65 to 70 %	5 to 45 °C		12'000 to 14'000	15 years	Long duration services
	Low	High	Low	High				Low	High	Low	High						
Lead-acid	1'419	1'792	380	448	Widely	Seconds	Minutes to a few hours	30 W/kg	50 W/kg	30 Wh/kg	50 Wh/kg	79 to 85 %	18 to 45 °C		500 to 1'000	12 years	Off-grid applications

For a more in-depth understanding of the technical properties and the cost of the different battery technologies, the reader is encouraged to review the thorough reports [11] and [15].

2.2.7 State of Charge (SoC)

The State of Charge (SoC) of a battery is a measurable value, that provides information about the level of available energy compared to the total capacity of electrical energy for the specific battery. More precisely the level of releasable capacity compared to the rated level of capacity, as shown in equation (2.1) [28].

$$SOC = \frac{C_{relesable}}{C_{rated}} \cdot 100\% \quad (2.1)$$

This terminology implies that the battery is fully discharged when $SOC = 0$, i.e., when $C_{relesable} = 0$ and that the battery is fully charged when $SOC = 100\%$, i.e., when $C_{relesable} = C_{rated}$. However, depending on the battery technology, the full capacity of a battery C_{max} may be different from the C_{rated} [28].

The SoC can also be expressed with a formula using the letter Q to represent the amount of charge, and where Q_n is the nominal or rated level of charge [29].

$$SOC(t) = \frac{Q(t)}{Q_n} \cdot 100\% \quad (2.2)$$

In the same way as the SoC can be quantified, the Depth of Discharge (DoD) can be expressed by using an equation showing how much of the total capacity that has been used, or released, from the battery. $C_{released}$ is introduced [28].

$$DOD = \frac{C_{released}}{C_{rated}} \cdot 100\% \quad (2.3)$$

2.3 HVDC Technology & HVDC Systems

High Voltage Direct Current (HVDC) systems is an evolving technology that has been developed and adapted to meet the technical and economic needs, both for today and for the years to come. So far, several hundred HVDC transmission systems are already commissioned, in operation or under ongoing construction around the globe [30].

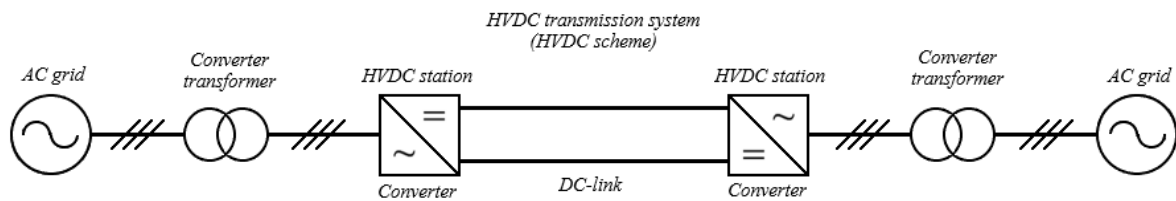


Figure 2.19: Illustrating an HVDC scheme or HVDC transmission system, including converter transformers

The advantage of the HVDC technology, compared to traditional High Voltage Alternating Current (HVAC) transmission systems, are mainly lower power losses for long-distance transmissions, higher controllability for the systems and that it enables the possibility to interconnect asynchronous bulk power systems [30].

The HVDC technologies can be divided into Line Commutated Converters (LCC) and Voltage Source Converters (VSC), where the VSC's can be divided into more applicable subcategories [30].

2.3.1 Line Commutated Converters (LCC)

LCC-HVDC's often referred to as "HVDC Classic", are based on thyristor technology and have a high power and voltage rating [30]. However, LCC-HVDC's are dependent of having an external AC grid voltage connected to its terminals and do therefore not provide any black start capability [30].

LCC-HVDC is a mature technology with high reliability. The control is based on the firing angle control, for both the inverter and rectifier side of the HVDC scheme [30].

Weaknesses for the LCC-HVDC's are considered to be the dependency of an external AC grid voltage, and the required strength of the external AC grid [30]. Furthermore, high reactive power consumption at levels around 50 to 60 % of the transmitted active power, in addition to high AC and DC harmonics that requires passive filtering, are considered to be drawbacks for this technology [30].

The LCC-HVDC have a unidirectional active power flow and the converters do only have the capability to consume reactive power from the connected AC grid [30]. This is illustrated in figure 2.20.

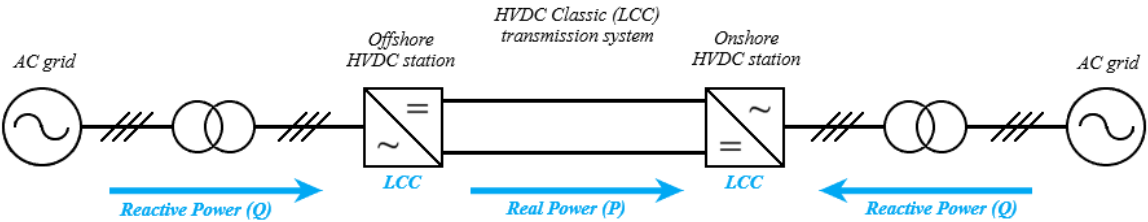


Figure 2.20: Illustrating the active and reactive power flow for an LCC-HVDC

2.3.2 Voltage Source Converters (VSC)

Voltage Source Converters (VSC) are relying on Insulated Gate Bipolar Transistors (IGBT's), operates at higher frequencies based on Pulse-Width Modulation (PWM), and has the possibility to keep the DC voltage stable under normal operating conditions [30].

Unlike the LCC-HVDC, the VSC-HVDC have the possibility to turn on and off the current at any given time, independently of the AC grid voltage, which enables more possibilities for the VSC-HVDC's [30]. As an example, will the VSC-HVDC have the capability to independently control the active power and the reactive power [30].

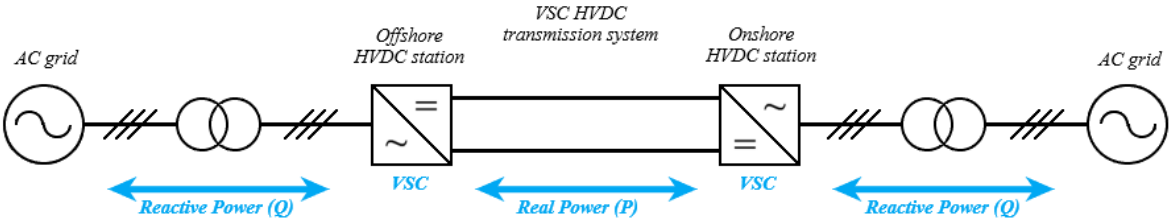


Figure 2.21: Illustrating the active and reactive power flow for a VSC-HVDC

The simplest form of VSC-HVDC, is the two-level VSC (2L-VSC), which historically has accounted for the largest share of commissioned HVDC-VSC's [30]. For the 2L-VSC the AC terminal voltage is created by switching between two voltage levels that corresponds to the negative and positive voltages on the DC bus terminals [30].

As the 2L-VSC creates high amounts of harmonic distortion, passive filtering equipment are needed to filter these harmonics [30]. The three-level VSC (3L-VSC) has been commissioned for some HVDC schemes and the 3L-VSC have better harmonic performance than the 2L-VSC, as the 3L-VSC have an additional zero-voltage step in the switching [30].

2.3.3 Modular Multilevel Converters (MMC)

The Modular Multilevel Converter (MMC) is a type of Voltage Source Converters (VSC), furthermore the MMC is both the newest VSC technology, the most promising VSC technology and now also starting to be the most common VSC technology for HVDC transmission systems [30, 31].

The MMC-HVDC poses several improvements from the 2L-VSC, including lower losses, significant lower level of harmonics and better blocking capabilities [31].

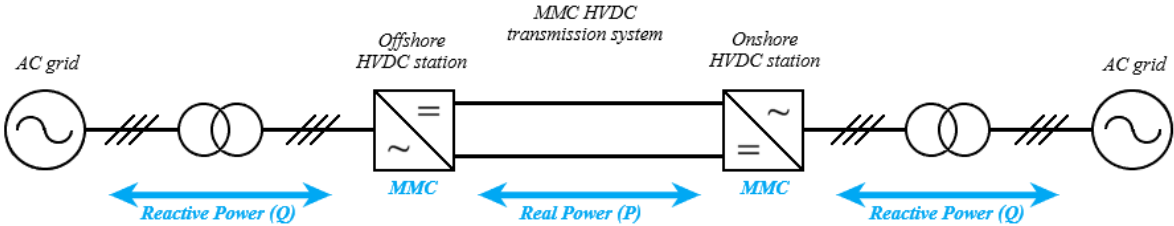


Figure 2.22: Illustrating the active and reactive power flow for an MMC-HVDC

Whereas the 2L-VSC do block the voltage for each phase-leg and acts like a few voltage sources, the MMC consists of several power modules in series for each phase leg. The power modules act like many voltage sources connected in series, where it is possible to turn them on and off independently [31].

The series connected power modules and their control, enables the possibility to build the AC waveform in steps and which results in an output that is closer to a filtered AC waveform [31]. More power modules will make each step smaller, the waveforms become closer to a sinusoidal waveform and the harmonics are reduced accordingly [31].

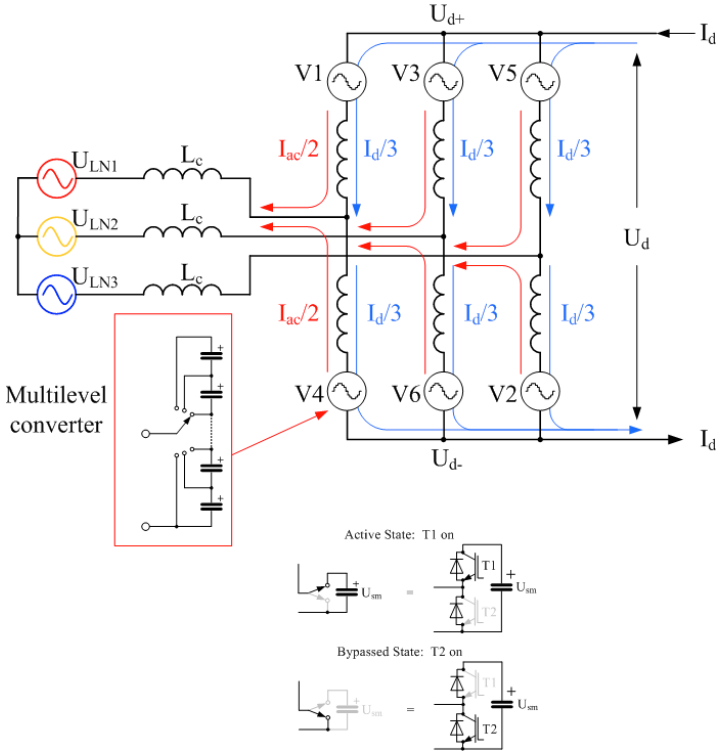


Figure 2.23: Principle for a Modular Multilevel Converter. Source: Wikimedia Commons [32]

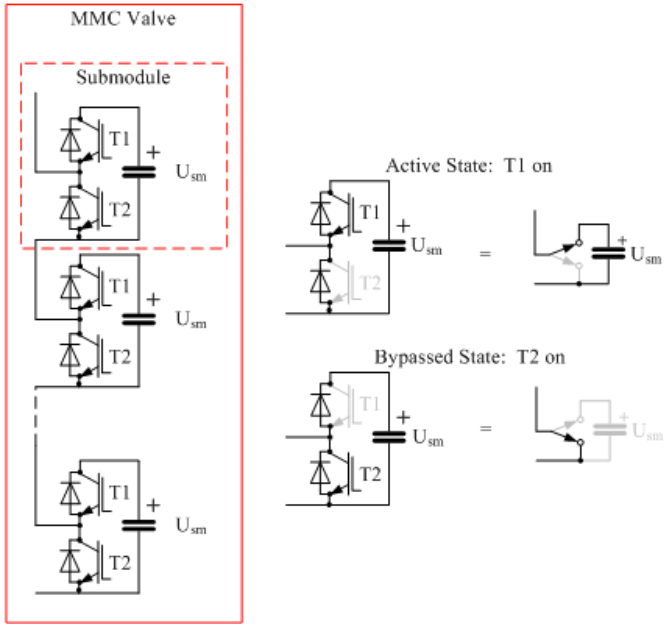


Figure 2.24: Modular Multilevel Converter. Submodule states. Source: Wikimedia Commons [33]

2.3.4 Available HVDC solutions in the market

A search to identify existing commercially available HVDC products in the market has been performed. The result is put into table 2.6. It is important to note that this overview is not considered to be exhaustive with regards to all available HVDC suppliers in the market. Furthermore, it is important to note that this report is not intended to compare or favorize any commercially available HVDC product. The sole purpose is to identify one or more commercially available products that satisfies the intended usage.

Table 2.6:
Available HVDC VSC products in the market, [34, 35, 36]:

Manufacturer	Product name	Technology
Siemens Energy [34]	HVDC PLUS [®]	VSC, MMC
Hitachi Energy [35]	HVDC Light [®]	VSC, MMC
GE Grid Solutions [36]	MaxSine [™]	VSC, MMC

It is decided not to describe any technical details or adapt any figures from the individual HVDC supplier web pages. This to avoid issues with regards to Copyrights and Intellectual Properties (IP's).

Available information can be accessed on the respective supplier web page and in brochures available at the mentioned web page [34, 35, 36].

In general, it is observed that the commercially available VSC MMC HVDC products have the grid stabilization services described in chapter 2.1.5, 2.1.6 and 2.1.7 of this report. E.g., grid-forming operation, black-start capabilities and reactive power support.

Furthermore, both HVDC Classic (LCC) and VSC MMC was observed on the web pages, but other types of VSC's, like 2L-VSC and 3L-VSC was not observed [34, 35, 36]. Only the VSC products were included in table 2.6, as this is the only technology relevant for further assessment in this thesis.

2.3.5 Offshore Wind HVDC Reference Projects

A search for relevant newer offshore wind HVDC projects has been performed. This to enlighten the understanding about the size, dimensions, and voltage levels for such projects.

Table 7.1 [37] in [31] are presenting the capacity and the DC-link voltage for several TenneT MMC-HVDC projects. These eight projects have a capacity between 576 MW and 916 MW and most of them a capacity around 800 to 900 MW [37]. Furthermore, the DC-link voltage is observed to be 320 kV for six of these eight projects, 300 kV for one project and 250 kV for one project [37].

Another reference project will be the Dogger Bank Wind Farm [38]. This is an ongoing project consisting of three offshore wind farms, Dogger Bank A, B and C, and where each farm will have an installed generation capacity of 1.2 GW [38].

The Dogger Bank A and B will have a combined capacity of 2,4 GW and be connected to an existing substation nearby Yorkshire [38]. The Dogger Bank C, with a capacity of 1.2 GW, will have a separate point of connection to the onshore AC bulk power system, as this wind farm will be connected to an existing substation at Teesside [38].

A separate project, the Sofia project, will have an installed capacity of 1.4 GW and the onshore HVDC converter will be located relatively close to the onshore Dogger Bank C converter, and be connected to the existing Teesside substation [39].

It is thus observed that the two onshore HVDC converters for Dogger Bank A and B will be located close to each other. Furthermore, that the two onshore HVDC converters for Dogger Bank C and Sofia will be located close to each other.

HVDC converters located in the near vicinity of each other, may lead to control interactions between the HVDC systems [40].

As this report will not review or explain the negative- or harmonic control interaction between converters or the need of dynamic performance studies (DPS), this scope of work will be mentioned in chapter 6 as an item of further work.

It can also be mentioned that “hybrid cables” may be considered for offshore wind HVDC schemes in the future, where the system is connected to two or more onshore stations [41].

2.4 Battery Energy Storage Systems (BESS)

The usage of Energy Storage Systems (ESS) has emerged during the recent years as this is considered to be a key enabler for the integration of RES [3, 42, 43].

Different ESS comes with different technologies and different properties, where some technologies has been known for decades and where some technologies are new and emerging [3, 42, 43].

The ESS technologies can be broken down to categories and subcategories. In the spectrum of mechanical ESS technologies, pumped hydro storage (PHS), compressed air energy storage (CAES) and flywheel energy storage (FES) can be found [3, 42, 43]. In the electric and magnetic category, supercapacitor energy storage (SCES) and superconducting magnetic energy storage (SMES) can be found [3, 42, 43]. Furthermore, battery energy storage (BES) and flow battery energy storage (FBES) are located in the electrochemical spectrum of energy storage technologies [3, 42, 43].



*Figure 2.25: Showing a picture of the Tehachapi Energy Storage Project (TSP).
Source: Wikimedia Commons [44]*

2.4.1 BESS Technologies

A typical BESS solution is consisting of a DC/AC converter topology and a transformer for the connection to the AC grid and a set of battery modules for the battery storage [42]. The battery modules can have the form as standardized containers, to achieve economies of scale, to ease transportation and to enable scalability [42].

The BESS converter topology can be both a single-stage DC/AC power conversion or a two-stage conversion where a DC/DC VSC converter topology is added in between the DC/AC converter and the battery [3]. The pros of having an additional DC/DC VSC converter, will be the extra controllability with regards to the DC voltage on the battery terminals [3]. As the DC voltage for an DC/AC VSC converter need to be as high as the peak-to-peak AC voltage, it will not be possible to deeply discharge a battery that is designed for such a usage, i.e., such a deep discharge [3]. The controllability of the two-stage VSC solution with a DC/DC converter enables possibilities for more advanced control functionalities, to better utilize the stored energy in the battery and to optimize charge cycles [3].

Figure 2.26 is showing the principles for a single-stage DC/AC VSC and a two-stage VSC consisting of a DC/DC VSC and a DC/AC VSC. Figure 2.26 is an adaption of the block diagram used for HVDC schemes in this thesis but inspired by the data in [3].

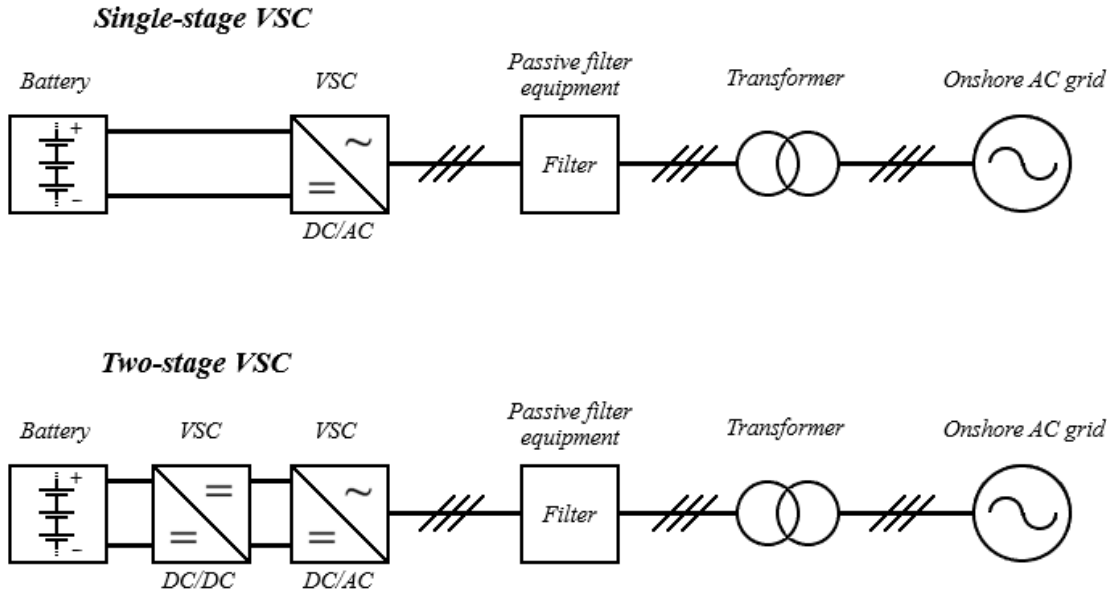


Figure 2.26: Single-stage and two-stage VSC for BESS application

2.4.2 Available BESS solutions in the market

A search to identify existing commercially available Grid-Scale BESS products in the market has been performed. The result is put into table 2.7. It is important to note that this overview is not considered to be exhaustive with regards to all available BESS suppliers in the market. Furthermore, it is important to note that this report is not intended to compare or favorize any commercially available BESS product. The sole purpose is to identify one or more commercially available product that satisfies the intended usage in this thesis.

Table 2.7:

Commercially available BESS products in the market, [45, 46, 47, 48, 49, 50, 51, 52, 53, 54, 55, 56, 57, 58, 59]:

Manufacturer / Supplier	Product name / Description	Link
Siemens Energy [45]	SIESTART™	https://www.siemens-energy.com/global/en/offerings/storage-solutions/battery-energy-storage.html
Hitachi Energy [46]	e-mesh™ PowerStore™	https://www.hitachienergy.com/offering/solutions/grid-edge-solutions/our-offering/e-mesh/powerstore
GE [47]	GE's Reservoir Solutions	https://www.ge.com/renewableenergy/hybrid/battery-energy-storage
Fluence [48]	Gridstack™	https://fluenceenergy.com/energy-storage-technology/gridstack-grid-energy-storage/
Tesla [49, 50]	Megapack	https://www.tesla.com/megapack and https://www.tesla.com/utilities
FlexGen [51]		https://flexgen.com/utility/
Wärtsilä [52]	GridSolv Quantum	https://www.wartsila.com/energy/solutions/energy-storage
Powin [53]	Centipede™	https://powin.com/products/hardware/
LG Energy Solution [54, 55]	LG Energy Solution Vertech	https://lgensol-vt.com/ and https://lgensol-vt.com/solutions/hardware-details/
SMA Sunbelt Energy [56]		https://www.sma-sunbelt.com/
Sungrow [57]		https://en.sungrowpower.com/solutionsDetail/11
Nidec [58]		https://www.nidec-industrial.com/markets/battery-energy-storage-solutions/
NGK Insulators [59]	NAS® Batteries	https://www.ngk-insulators.com/en/product/nas.html

It is decided to not describe any technical details, reveal any data, or adapt any figures from the individual BESS supplier web pages. This to avoid issues with regards to Copyrights and Intellectual Properties (IP's). Available information can be accessed and assessed by using the different links in table 2.7.

The search for commercially available BESS's in the market resulted in many available solutions. It is assumed that the available solutions listed in table 2.7 only are showing a fraction of the available solutions and suppliers in the market as of 2022.

It is observed a variation in the level of available technical data for the different BESS manufacturers. In general, functionalities, scalability and main services are mentioned, but not detailed technical information about the components, converter topologies, controllers, or software. This may be "black-boxed" due to proprietary rights, IP's, and commercial considerations.

An observation is that the AC voltage is relatively low, for the products where this is described, and that this voltage must be transferred to higher voltage levels by using transformers. AC voltage levels around 400 V, 480 V and 690 V are observed.

Furthermore, it is in general observed that several of the BESS providers are describing power system stabilizing services that are mentioned in chapter 2.1.5, 2.1.6 and 2.1.7 in this report.

2.4.3 Large-Scale Grid Stabilizing BESS Reference Projects

An extensive search for large-scale, or utility-scale, BESS's has been performed. This search for reference projects has been mainly focused on finding projects which are realized with the purpose to provide services of power system stability, that has a significant power capacity and that are transferrable to the usage in this thesis. Many projects have been reviewed but not mentioned in this report, as their primary function is long term energy storage, are too small or consists of many distributed plants.

One reference project will be the Hornsdale Power Reserve, operated by Neoen and co-located with the Hornsdale Wind Farm [20]. This BESS project was commissioned and put in operation in November 2017 and had a rated capacity of 100 MW and 129 MWh [20]. In September 2020 an upgrade was finalized, adding 50 MW / 64.5 MWh, so that the total power capacity reached 150 MW [20].

Furthermore, this upgrade in 2020 contained some upgrade to the control as well. A Virtual Machines Mode developed by the BESS manufacturer was activated, so that the whole 150 MW BESS plant got the capability to provide services of inertia to the power system [20].

As already mentioned in chapter 2.1.8, the Hornsdale Power Reserve has prevented a disconnection of the South Australian power system from the larger Australian Power System, at least two times, when a contingency event has occurred on the grid [11].

Another reference project will be the Victorian Big Battery, also operated by Neoen [21]. The Victorian Big Battery have a capacity of 300 MW / 450 MWh, is supplied by the same manufacturer as for the Hornsdale Power Reserve and is consisting of 210 BESS packages [21]. The Victorian Big Battery is strategically located side by an existing high voltage transmission hub and will help supporting the transition to clean renewable energy [21].

2.5 BESS for HVDC

2.5.1 BESS connected to the DC link

In this literature review it has not been identified commissioned HVDC schemes where a BESS is connected to the DC link of an HVDC system.

However, it does exist literature which make it feasible to analyze such a solution. An example will be the NTNU Master Thesis *Use of Battery Energy Storage for Power Balancing in a Large-Scale HVDC Connected Wind Power Plant* [42] from 2017, which is assessing the feasibility to connect a BESS to the DC link of an HVDC scheme.

The main objective of that project was to show that a battery connected to the DC link of an HVDC transmission system, transferring power from an offshore wind farm to the onshore grid, can provide ancillary services of primary and secondary reserves for onshore grid stabilization [42].

With regards to the selection of a DC/DC converter topology, it is observed that a soft switched Dual Active Bridge (DAB) converter was concluded to be the most optimal choice of converter, but that a MMC converter was finally selected [42]. The MMC was finally concluded to be the best option as the MMC was available in the industry and as the MMC was the converter topology that performed best in most of the criteria for the mentioned project [42].

Two converters could have been connected in a front-to-front DC/AC/DC configuration, without galvanic isolation. It was decided to have a galvanic isolation on the AC side in between the converters as this galvanic isolation will prevent a direct current path between the converters [42].

In that project it was selected a MMC for the connection to the DC link of the HVDC system and a two level VSC for the connection to the battery. It was clearly stated that it would be a better option to use two MMC's with regards to performance, and possible provision of distributed batteries, but that a 2L-VSC was selected to simplify simulations and as it would not have significant impact on the desired result [42].

As the 2L-VSC with series connected IGBT's has some limitations with regards to upper voltage levels, the transformer used for galvanic isolation will enable the possibility to have a lower voltage 2L-VSC AC-terminal side [42].

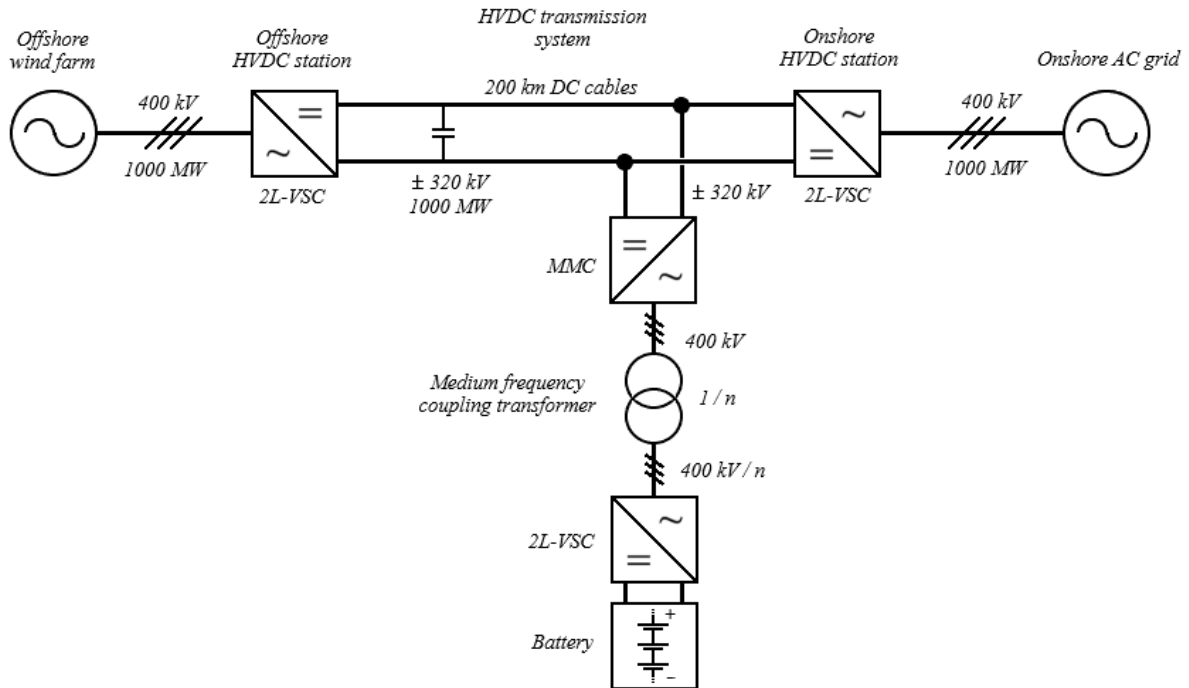


Figure 2.27: Block diagram of the HVDC scheme and BESS used in the reviewed Master Thesis. Recreated based on Figure 1.1 in [42]

The battery storage system EssPro™ from ABB was selected for the battery part [42]. The different BESS solutions available in the market, normally consist of battery containers, DC/AC converters and transformers to be able to connect the battery to the AC grid. In that project, only the battery container part (battery module) of the EssPro™ was used [42].

The EssPro™ battery container supports different battery technologies and in that project the lithium-ion battery technology was used. The voltage of one battery container was assumed to be at the max level, i.e., $V_{module} = 1.2 \text{ kV}$, as the battery in total will be very large to achieve a capacity of 180 MW, and as the battery voltage is dependent on the voltage of the 2L-VSC [42].

It was connected 273 EssPro™ battery containers (modules), where 91 containers were put in a series connection to achieve the proper voltage and with 3 containers in parallel to achieve the correct power [42]. This resulted in a battery pack with a power rating of 180 MW, a battery voltage of 108.87 kV, a battery current of 1653 A, a battery capacity of 413.25 Ah, a battery energy of 45 MWh, and with a discharge time equal to 15 minutes [42].

It was performed simulations in Simulink with scripts made in MATLAB. Main components have been simplified and the battery has been very simplified in the simulation model, as the battery is represented by an ideal DC voltage source in series with a small resistor [42]. That has been done as the main objective for the simulation was to show that it can be a bidirectional power flow to/from the battery, and as the objective was not to optimize the battery storage system with regards to efficiency, losses, and long lifetime [42].

The conclusion to the mentioned master's thesis was that the BESS connected to the DC link of the HVDC system can be used to provide ancillary services to the grid and support RES integration [42]. It was concluded that the lithium-ion battery technology was the most promising technology for the application in that project [42].

For the DC/DC converter it was concluded that two galvanically isolated front-to-front VSC's, where a medium frequency transformer was used for the galvanically isolation, was the optimal topology for that project [42]. The most optimal VSC technology commercially available in the market was concluded to be the MMC. Furthermore, it was noted that the MMC is a complex and expensive converter, and that it was discussed whether the DC/DC converter topology should be designed with two MCC's or not. It was concluded to use a 2L-VSC on the LV-side of the DC/DC converter and a MMC on the HV-side, in the mentioned project [42].

2.5.2 BESS connected to the AC grid side of the onshore Converter

It has been identified commercially available BESS solutions that can be connected to the AC grid side of the onshore converter. These are described in chapter 2.4 and can be connected to the AC grid independently of the HVDC system. It may even not be located close to the onshore converter building. However, it may be necessary to procure large numbers of these commercially available package solutions to achieve a large enough “headroom” for primary and secondary reserves.

In the NTNU Master Thesis *Battery energy storage connected to a three-phase 50 Hz grid* [43] from 2017, an MMC connected to a battery, used as a BESS, and connected to the AC grid side of the onshore converter, was assessed [43].

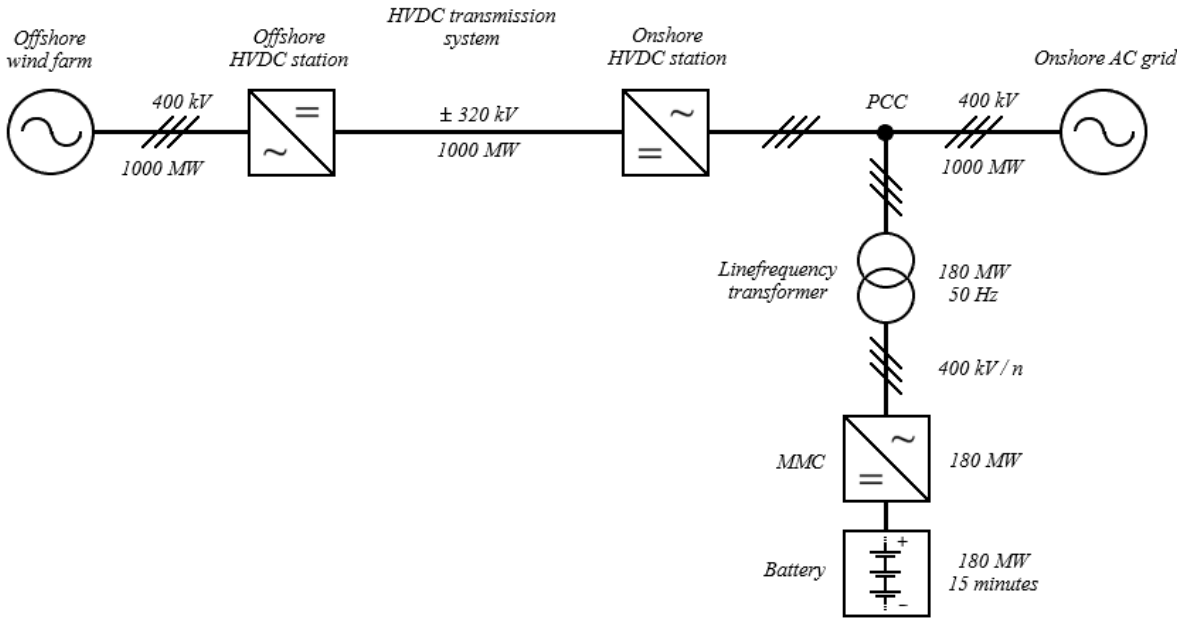


Figure 2.28: Single-line diagram of the HVDC scheme and BESS connection, used in the reviewed Master Thesis. Recreated based on Figure 1.1 in [43]

In this thesis the utilization of an MMC-BESS combined with a large amount of BESS battery packages, to provide ancillary services of primary and secondary reserves was assessed, simulated and proven. The setup used commercially available equipment [43].

3 Assessment of Solutions

In this chapter the assessments of solutions are performed. These assessments are based on the literature reviewed in chapter 2.

As described in chapter 1, the needs, requirements, and dimensioning criteria's had to be identified upon available literature, reference projects and commercially available solutions.

The review and data collection were performed in chapter 2. Chapter 3 is dedicated to the assessment of the collected data and the interpretation of possible solutions.

3.1 Dimensioning Criteria's

It is given that an HVDC system is to be connected to an offshore wind farm. Furthermore, that an electrochemical energy storage shall be connected to the HVDC system or to the onshore AC grid, to provide ancillary services of primary and secondary reserves.

Ancillary services, traditional power system stability services, primary control, secondary control, and operational reserves are thorough reviewed in chapter 2.1.1 to chapter 2.1.3 and should have enlightened the readers understanding about power system stability and the needs with regards to reserves.

In chapter 2.1.3 it is described that the spinning reserves normally have the capacity of 15 to 20% of the base load [3].

The capacity of this traditional spinning reserve is considered to be transferrable to the required capacity of the electrochemical energy storage reserve, as the required amount of active power and the required amount of energy, to restore the frequency by injecting active power into the power system, will be the same regardless of the control technology used in the IBR.

It is though noted that the electrochemical storage technology should have a very rapid response time and be able to deliver high rates of power, i.e., to have a high power capacity and the ability to dispatch large amounts of energy at short timeframes. This to utilize the services reviewed in chapter 2.1.5, 2.1.6 and 2.1.7, where the mentioned control services operate very fast and requires a high power capacity and a quick battery response time, to compensate for the lower grid inertia.

The Fast Frequency Response (FFR) operates much quicker than traditional Primary Frequency Response (PFR) and will require a high power dispatchability and a quick response time to inject large amounts of active power into the power system. As reviewed in chapter 2.1.5 and 2.1.6, is the FFR control functionality available both for GFL IBR's and GFM IBR's.

More advanced GFM control functionalities reviewed and described in chapter 2.1.7 will also require a quick response time and a substantial power dispatchability, as these virtual control functionalities to emulate inertia or to emulate synchronous generators (VSM's), will require power injection from the moment a contingency occurs, to fully mimic a real inertial response.

When assessing the data reviewed in chapter 2.3.4, which will be the search after commercially available HVDC solutions in the market, it is observed that the identified manufacturers can supply the HVDC Classic (LCC) and MMC-HVDC (VSC), where only the MMC-HVDC is relevant for the usage in this thesis. Furthermore, it is not observed easily available information about other VSC's like the 2L-VSC on their respective webpages. This may be indicating that the 2L-VSC and similar topologies are obsolete, from a commercial point of view.

This observation deviates a little bit from the 2017 Master theses assessed in chapter 2.5, where the MMC-HVDC was deemed to be the most promising technology from a technical point of view and with regards to efficiency, but where the 2L-VSC was considered to be a more low-cost and easier achievable solution. Furthermore, this observation may be an indication of the rapid technology development in this field of power electronics.

The MMC-HVDC technology is selected as the HVDC converter topology in this thesis, due to its technical capabilities, the commercial availability and for the maintainability and availability in the years to come.

When assessing the reviewed data in chapter 2.3.5, it can be observed that the power capacity is varying in between 800 to 1'400 MW for newer HVDC projects connected to large scale offshore windfarms, furthermore that the DC-link voltage in many cases is 320 kV.

As a result of this observation, the HVDC-link in this project can be assumed to have a rated power capacity equal to 1000 MW and a DC-link voltage equal to 320 kV.

To summarize, the HVDC scheme in this thesis will consist of one onshore MMC-HVDC converter, one offshore MMC-HVDC converter, have a rated DC-link voltage of 320 kV and a rated power of 1000 MW.

To achieve an ancillary reserve with a power capacity equal to 15 to 20% of the base load, the electrochemical storage must have a rated power capacity between what is shown in equation 3.1 and equation 3.2.

$$P_{BESS_{min}} = P_{HVDC} \cdot 15\% = 1000 \cdot 15\% = 150 [MW] \quad (3.1)$$

$$P_{BESS_{max}} = P_{HVDC} \cdot 20\% = 1000 \cdot 20\% = 200 [MW] \quad (3.2)$$

The discharge time at maximum power output, which together with the selected power capacity will make up the required energy capacity, should at least be 10 minutes to cover the role as a secondary reserve. Reference is made to chapter 2.1.1 where literature describing the timeframes for different ancillary services is assessed.

The discharge time at maximum power output can with advantage have some headroom, both to enable the possibility for services of longer durations, but most important to avoid deep cycling when executing the main tasks as primary and secondary reserves. As reviewed in chapter 2.2, may deep cycling reduce the lifetime of the battery, depending on the selected battery technology and chemistry. Therefore, the minimum recommended duration at maximum power output is extended to 15 minutes.

3.2 Electrochemical Storage Technology

In this chapter the electrochemical storage technology is assessed. This assessment is based upon the literature review in chapter 2.2 and the requirements derived in chapter 3.1.

To summarize, it is so far decided that the rated power capacity of the electrochemical energy storage must be in between 150 and 200 MW, and that the battery must sustain a discharge current at the rated power output level, for 15 minutes. Furthermore, that the battery must have a quick response time to enable the possibility for the needed services.

Other factors that are of interest, will be power density and energy density, the cost related to power capacity and energy capacity, the reliance of scarce materials, lifetime and other technical properties that is relevant for the intended usage.

When it comes to cost, it is in general in the reviewed literature in chapter 2.2, shown that the cost rate per unit of power capacity (\$/kW) is much higher than the cost rate per unit of energy (\$/kWh). As the energy storage considered in this thesis have a very high power rating and in general terms a shorter duration, due to the objectives of providing ancillary services, the cost rate per unit of power capacity (\$/kW) will reflect the actual cost.

Another important factor would be the matureness of the technology and examples of commissioned deployments of the technology, as this gives an indication about the availability, maintainability, reliability and in general the feasibility for project execution within the nearest future.

The lithium-ion battery technology is reviewed in chapter 2.2.2. This is the reviewed battery technology with the highest power density, without any competing technologies within reach. The energy density is very high, the round-trip efficiency is good, and the reaction time is at a sub-second to second level, which should suit the need. This technology is widely commercialized, and it is put in operation plants which exceed the required power capacity identified in this thesis.

The lithium-ion battery has sub-categories, where the NMC is the most used as per today, but where the LFP is considered to be more popular in the years to come.

The sodium-sulfur battery technology is reviewed in chapter 2.2.3. This battery technology has a very high energy density, almost at the levels for lithium-ion batteries, but a much lower power density than the lithium-ion technology. The cost rate per unit of power (\$/kW) is significantly higher than for the lithium-ion. The high energy density and the capability to dispatch power at the maximum power output level for several hours, makes this a promising candidate for long-duration services.

The flow battery technology is reviewed in chapter 2.2.4. The flow battery technology has the lowest power and energy density of all assessed battery technologies, and the power density is significantly lower than for all other assessed technologies. However, this initially commercialized technology has a reaction time at the sub-second level and may be a promising technology for long-term storage in the future.

The lead-acid battery technology is reviewed in chapter 2.2.5. This is a widely commercialized technology and a well-known battery technology. The cost range per unit of power (\$/kW) is low and may even compete with the lithium-ion. However, the power density and energy density are quite low, and the reaction time is at a second level. The cycle life is also a bit low, compared to the other reviewed technologies.

Table 3.1:

Summary of the review in chapter 2.2, colored to highlight pros & cons

Battery technology	Cost range in USD per power unit (\$/kW)		Cost range in USD per energy unit (\$/kWh)		Commercial availability	Reaction time	Duration of discharge at max power capacity	Power density		Energy density		Round-trip efficiency	Operating temperature	Rate of self-discharge	Cycle life (# of cycles)	Expected lifetime	Foreseen usage next decades
	Low	High	Low	High				Low	High	Low	High						
Lithium-ion in general	1'302	1'947	352	487	Widely	Sub-seconds to seconds	Minutes to a few hours	4'000 W/kg	6'500 W/kg	210 Wh/kg	325 Wh/kg	86 to 88 %	-20 to +65 °C		1'000 to 2'000	10 years	Increasing
NMC	1'320	1'827			Widely			6'500 W/L		325 Wh/L			-20 to +55 °C	1% per month	around 1'200		Declining compared to NCA/LFP
NCA					Widely			4'000 W/L	5'000 W/L	210 Wh/L	600 Wh/L		-20 to +60 °C	2 to 10 % per month	above 1'000		Increasing
LFP	1'302	1'752			Widely			4'500 W/L		220 Wh/L	250 Wh/L		-20 to +60 °C	1% per month	around 2'000		Increasing
	Low	High	Low	High				Low	High	Low	High						
Sodium-sulfur	2'394	5'170	599	1'293	Initial	Sub-seconds	Several hours	120 W/kg	160 W/kg	150 Wh/kg	240 Wh/kg	77 to 83 %	300 to 350 °C	Very low	around 4'500	15 years	Long duration services
	Low	High	Low	High				Low	High	Low	High						
Flow batteries	1'863	2'438	499	609	Initial	Sub-seconds to seconds	Several hours	0.5 W/kg	2 W/kg	10 Wh/kg	50 Wh/kg	65 to 70 %	5 to 45 °C		12'000 to 14'000	15 years	Long duration services
	Low	High	Low	High				Low	High	Low	High						
Lead-acid	1'419	1'792	380	448	Widely	Seconds	Minutes to a few hours	30 W/kg	50 W/kg	30 Wh/kg	50 Wh/kg	79 to 85 %	18 to 45 °C		500 to 1'000	12 years	Off-grid applications

Table 3.1 is an update of table 2.5, where some of the main data from the review in chapter 2.2 has been colored to highlight pros & cons of relevant properties for the decision making.

The most promising candidate reviewed in this thesis will be the lithium-ion battery technology. The matureness of the technology, the experience from commissioned projects, the proven results, the technical properties with regards to this short-duration high-power usage, the cost range for high-power solutions and the overall impressions compared to the other technologies, makes this a clear choice.

More specifically the LFP chemistry seems to be the most promising candidate. This is a candidate that already is available and that will take over much of the lithium-ion market in the years to come.

When ensuring the shift to sustainable energy sources, it is also an objective to select sustainable technologies that to the extent possible do not rely on scarce or rare minerals.

As LFP is compatible with NMC with regards to technical properties and cost – and as LFP do not rely on Manganese or Cobalt – this makes LFP the recommended choice.

3.3 BESS connection to the HVDC system

In this chapter an assessment of the different possibilities for connection of a BESS to the HVDC system is performed. This assessment is based upon the reviewed data in previous chapters of this report and the assessment has a practical approach. The focus is at solutions that are deemed to be feasible to realize within the first years to come. The assessment is presented as separate cases, highlighting the feasibilities and the pros and cons for each individual case.

3.3.1 Case 1: Commercially available BESS connected to the AC grid

A solution by using commercially available BESS products is assessed. These commercially available BESS products were reviewed in chapter 2.4, with subchapters 2.4.1 to 2.4.3. Figure 3.1 gives an illustration of the point of connection to the system, which in this case will be the AC grid side of the onshore converter. Figure 3.1 is showing the principle and do not contain details, BESS transformers or HVDC converter transformers.

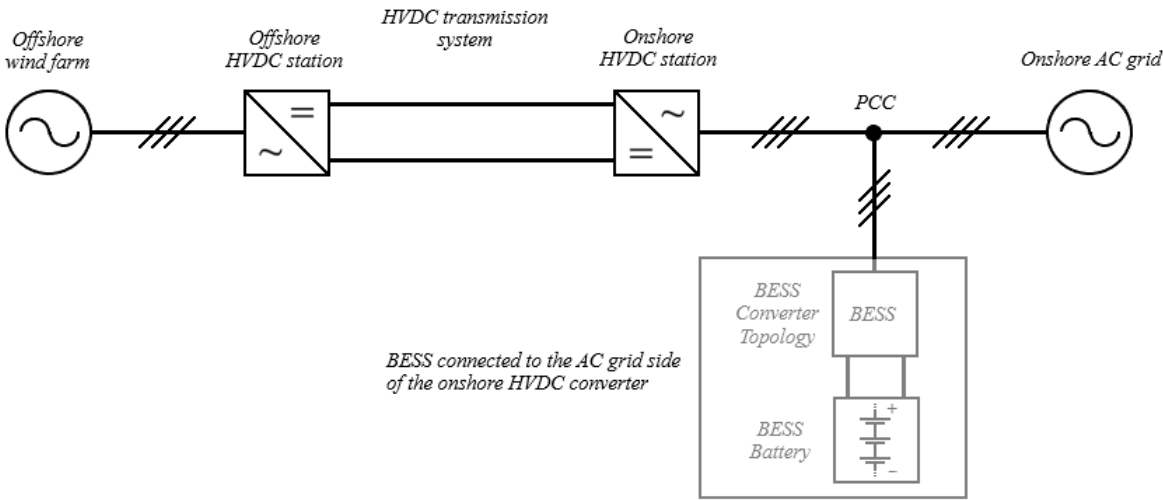


Figure 3.1: Block diagram showing the point of connection to the system

Commercially available BESS solutions are a type of technology that has already been commissioned, that has been in operation for years and the different solutions undergoes a rapid technology development with regards to functionality and efficiency. As it is many manufacturers and suppliers of these modular scalable BESS's, it is considered to be a high degree of competition and a continuously technology development among the different manufacturers. Furthermore, these BESS products are highly scalable, and some manufactures do even use the term “infinitely scalable” on their web pages.

However, the intended usage related to a large HVDC system, may require many individual BESS packages to cover the required level of power. Each BESS package will consist of an inverter and one or more battery modules. Depending on the selected manufacturer, it may be one LV-MV transformer for each inverter, or it may be connected several BESS packages to each LV-MV transformer.

Figure 3.2 is showing a block diagram illustrating BESS packages connected to the AC-grid side of the onshore HVDC converter and where each BESS package has an individual LV-MV transformer.

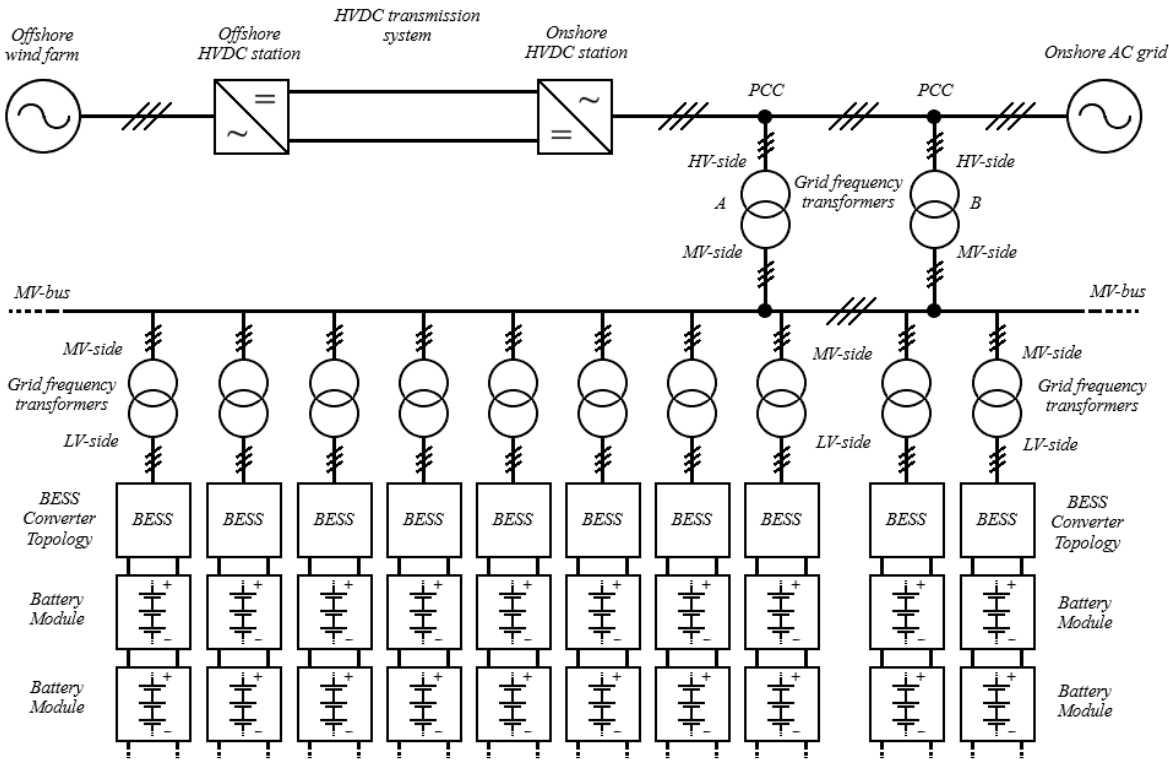


Figure 3.2: Block diagram that illustrates several BESS's connected to the AC-grid side

Figure 3.3 is showing the same concept as figure 3.2, but where BESS packages are sharing LV-MV transformers. It must be clearly stated that figures 3.2 and 3.3 are only illustrating the concept and that the final layout of transformer usage, voltage levels and connections will be highly dependent of the selected solution and the selected manufacturer.

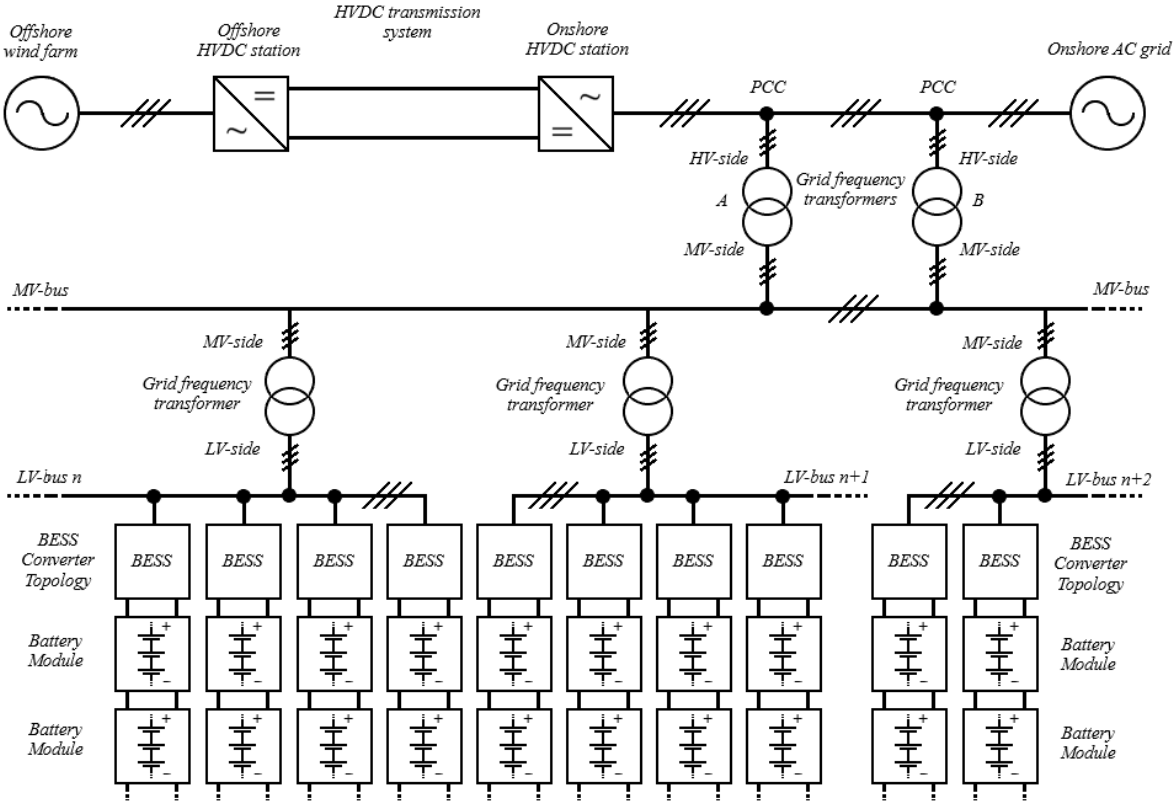


Figure 3.3: Block diagram that illustrates several BESS's connected to the AC-grid side

As observed in figure 3.2 and 3.3, these commercially available “packages” are very scalable and can be expanded if the need should change in the future. Furthermore, as the BESS packages are supplied as units and connected to the grid via transformers, which provides galvanically isolation, this should enable the possibility for multivendor solutions.

The large numbers of separate units will result in a highly redundant and maintenance friendly configuration with regards to avoiding outage when faults occurs or when doing scheduled maintenance where one or more BESS's must be electrically disconnected.

3.3.2 Case 2: MMC-BESS connected to the DC-link of the HVDC system

The literature review for connecting a BESS to the DC-link of the HVDC system was performed in chapter 2.5.1.

It was not identified any commissioned HVDC system where a BESS has been connected to the DC-link of the HVDC system.

A master thesis assessing the possibility of connecting a large BESS to the DC-link of a HVDC system, by using HVDC converters was identified and reviewed in chapter 2.5.1. The objectives of this master thesis were to prove the feasibility of connecting a BESS to the DC-link of a HVDC system to provide services of primary and secondary reserves, and to perform simulations to prove the feasibility of the bidirectional power flow needed. This was successful, but the models used was simplified to prove the working principles and cannot be used for comparison of state-of-the-art technologies with regards to efficiency.

For that mentioned master thesis, it was used 2L-VSC's for the HVDC link itself, a 2L-VSC for the BESS converter connected to the battery and an MMC-HVDC for the connection to the DC-link. It was though noted that two MMC's would be more efficient.

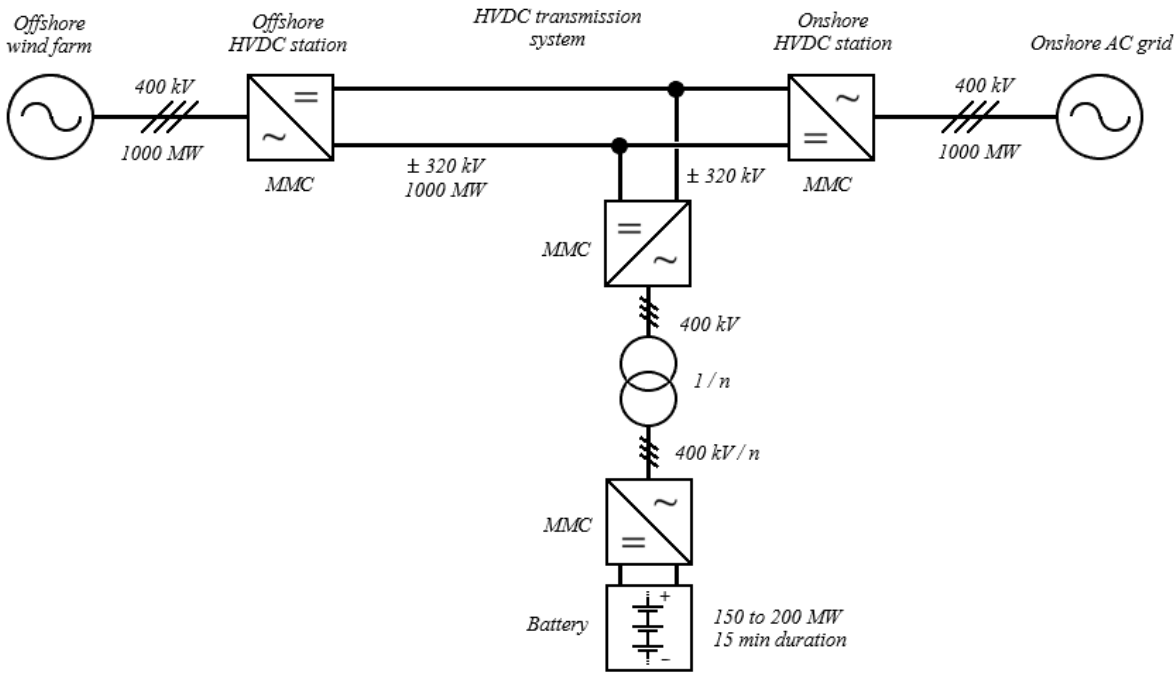


Figure 3.4: Single-line diagram of an MMC-BESS connected to the DC-link of the HVDC system

In chapter 3.1 it is concluded that an MMC-HVDC will be used for the HVDC converters in this thesis, that the rated power capacity will be 1000 MW and that the DC-link voltage will be 320 kV.

For connecting the battery storage to the DC-link, it is recommended to use two MMC-HVDC converters, where a transformer may be considered connected between the MMC-HVDC's to provide galvanic isolation. This is illustrated in figure 3.4.

The justification for using MMC-HVDC's are both based on the technical superiority of the MMC technology, described in chapter 2.3.3, the review of the master thesis in chapter 2.5.1, but most important the availability of commercial solutions reviewed in chapter 2.3.4.

In addition it is assumed that the "MMC-standardization" will have a positive contribution with regards to availability of spare parts, economies of scale, and a standardization of control system, SCADA, and Human Machine Interface (HMI) solutions.

As the MMC-BESS is connected to the DC-link of the HVDC-system and therefore is not facing the onshore AC grid directly, it must be the onshore MMC-HVDC connected to the onshore AC grid that provides the control functionalities with regards to power system stability.

The MMC-HVDC's do have a high level of control functionalities for power system stability and GFM operation. This can be accessed by using the references provided in chapter 2.3.4.

One side-effect of connecting the MMC-BESS to the DC-link of the HVDC system, would be that maintainability and availability. To provide services of primary and secondary reserves to the onshore bulk power system, both two MMC-BESS converters must be operating, in addition to the onshore MMC-HVDC.

If one of the three MMC-HVDC's trips, experiences a forced outage, or a service outage, the ancillary services provided to the onshore bulk power system will stop. This may in some cases be considered acceptable, but it may depend on geographical considerations, like described in chapter 2.1.8, and other external factors and requirements.

In case of a stepwise project development of several large-scale windfarms, like described in chapter 2.3.5, the BESS connection to the DC-link may have some constraints. This is illustrated in figure 3.5.

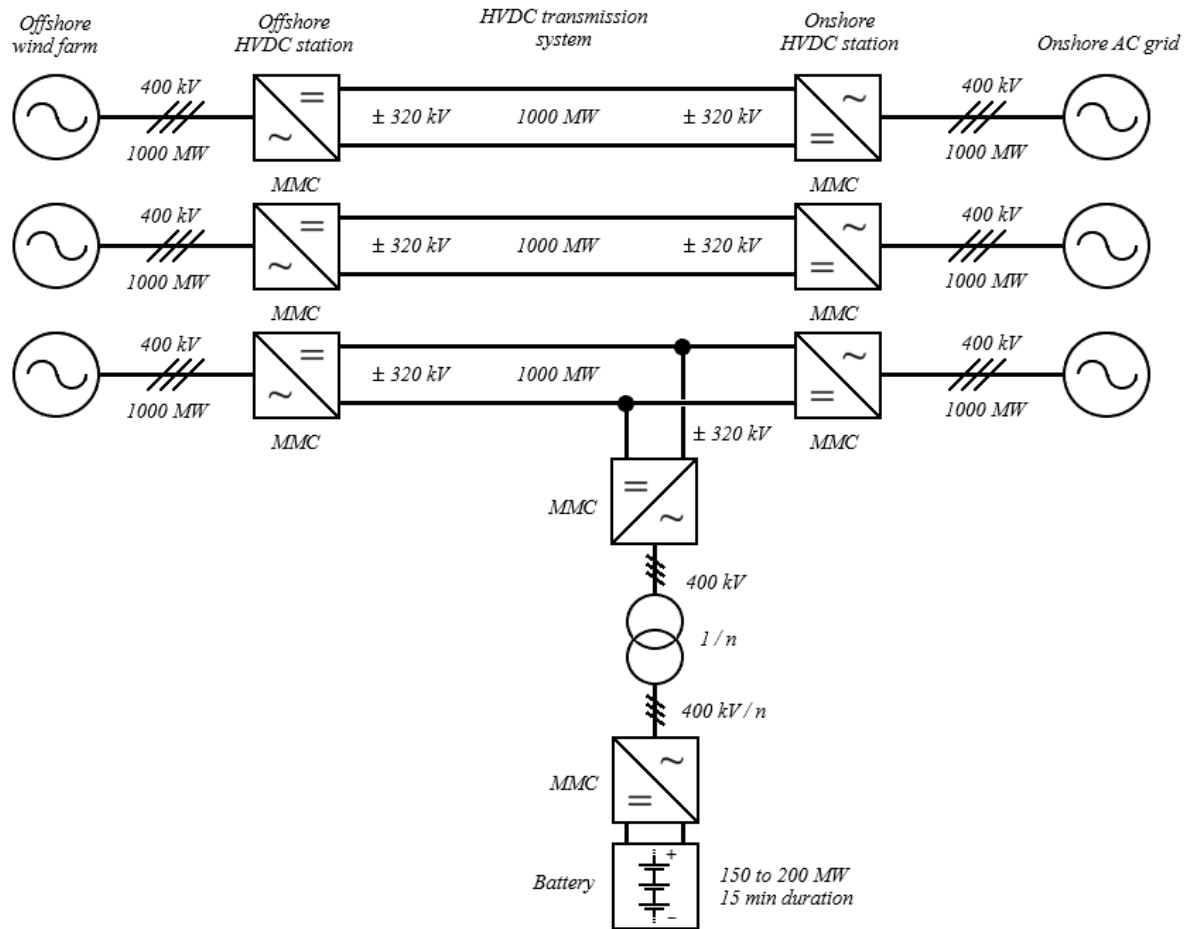


Figure 3.5: Single-line diagram of an offshore windfarm project developed in three project phases, where an MMC-BESS is connected to the DC-link for one of the HVDC's

Figure 3.5 is showing a stepwise project development of large-scale offshore windfarms relying on separate HVDC systems for connection to the onshore bulk power system.

For such an overall configuration, the connection to the DC-link for one of the HVDC's may have some drawbacks, and especially if the MMC-BESS is considered to provide ancillary services for all the HVDC's, as the services will highly rely on one of the HVDC systems with several possible "single point of failure".

However, it's though noted, that the capacity of the MMC-BESS in figure 3.5 is not large enough to cover the need for all three HVDC's.

An option would be MMC-BESS's connected to the DC-link for each HVDC system. This will increase the reliability, but will come with some additional cost, due to the increased amount of MMC's.

Another side-effect of having the MMC-BESS connected to the DC-link of the HVDC system, would be that the total amount of power from both the offshore wind farm and the battery storage will need to pass through the onshore HVDC converter. In the more unlikely event, where both the wind farm is operating at its maximum power output, and a contingency event occurs in the onshore bulk power system, the onshore converter will need to dispatch the additional power needed from the battery system.

The onshore converter must then be dimensioned for such an operation, i.e., have a rated power for this service, or the control must limit the ancillary service to only operate when it is enough capacity. This should be manageable in the HVDC control.

The solution will be dependent on however the MMC-BESS is deemed to provide ancillary services, for external contingency events, when the wind farm is operating at its maximum power output, or not. This scenario is illustrated in figure 3.6.

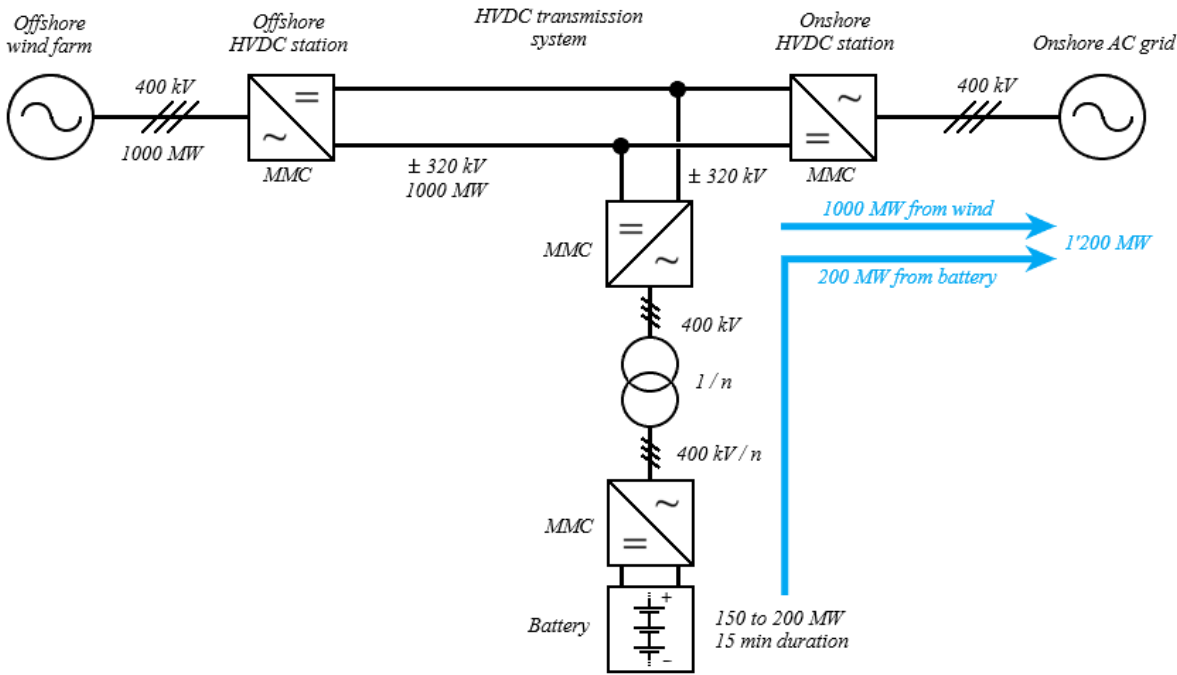


Figure 3.6: Single-line diagram of an MMC-BESS connected to the DC-link of an HVDC and where an external onshore contingency event occurs when the wind farm operates at maximum output

The connection of an MMC-BESS may seem more relevant for “hybrid cables” [41], which in this case will consist of an multiterminal HVDC scheme, with onshore HVDC converter stations at two separate locations and most likely in two separate countries.

Hybrid cables are explained in the following SINTEF web article [41], and as described in the article, this is a highly relevant scenario for upcoming large-scale HVDC offshore wind projects.

When connecting one or more MMC-BESS’s to a multiterminal DC-network, the storage solution will be able to provide power reserve for both receiving ends. The need of the reserve may be different for the two onshore converter stations. In addition, if one (or both) of the connected AC bulk power systems are considered to be very large and strong, the interconnected power systems may work as a reserve by itself.

The principle of connecting an MMC-BESS to a multiterminal HVDC scheme with hybrid cables is shown in figure 3.7.

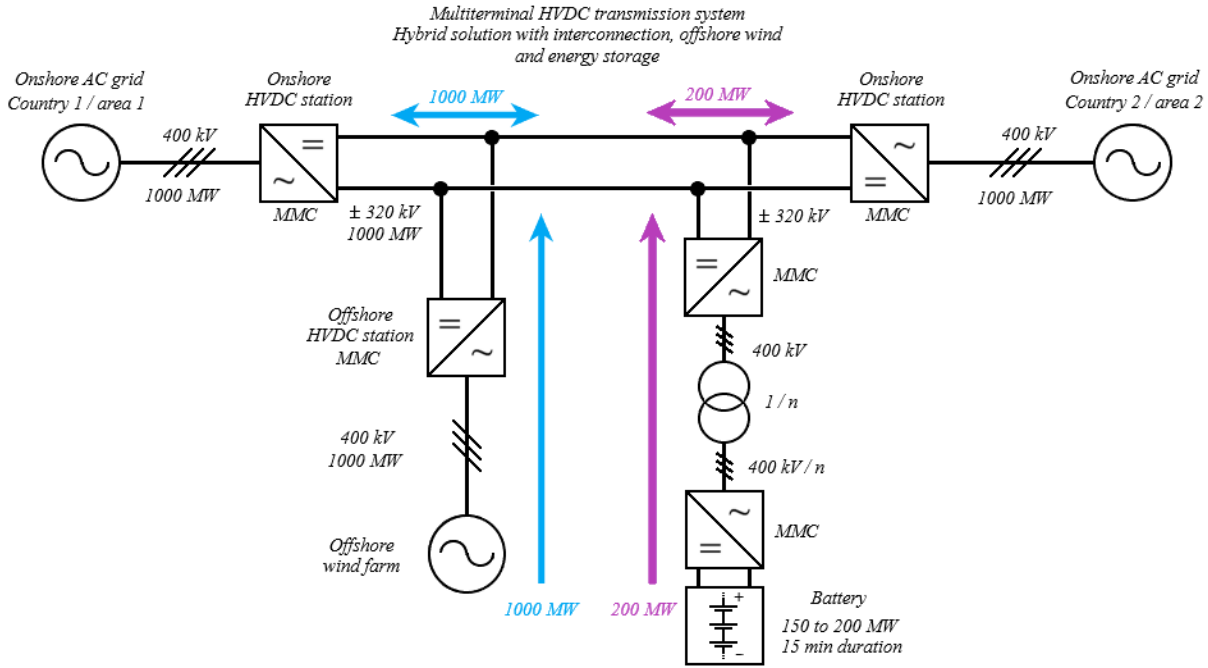


Figure 3.7: Single-line diagram of a multiterminal HVDC scheme with “hybrid cables” and an MMC-BESS connected to the DC-link

3.3.3 Case 3: MMC-BESS connected to the onshore AC grid

The literature review for connecting an MMC-BESS to the AC-grid side of the onshore HVDC converter was performed in chapter 2.5.2.

It was not identified any commissioned system where an MMC-HVDC converter has been used for a large-scale BESS solution.

When it comes to connection of BESS solutions to the onshore bulk power system, any commercially available solution reviewed in chapter 2.4 could be considered. As this is assessed in chapter 3.3.1, the assessment in chapter 3.3.3 will be dedicated to the utilization of a large-scale BESS relying on an MMC-HVDC.

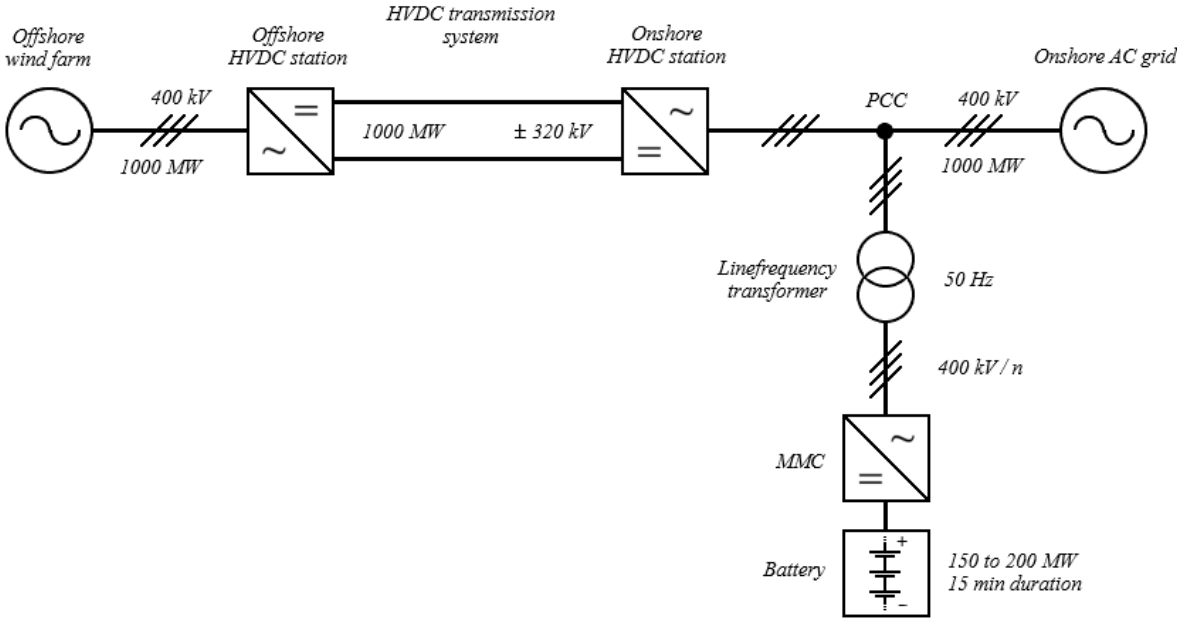


Figure 3.8: Single-line diagram of the HVDC scheme and MMC-BESS connection

The MMC-BESS connected to the AC grid side of the onshore HVDC converter, will not rely on the onshore HVDC converter itself and would therefore have less possible single point of failure and a scalable MMC-BESS would enable the possibility for a common storage reserve, as shown in figure 3.9.

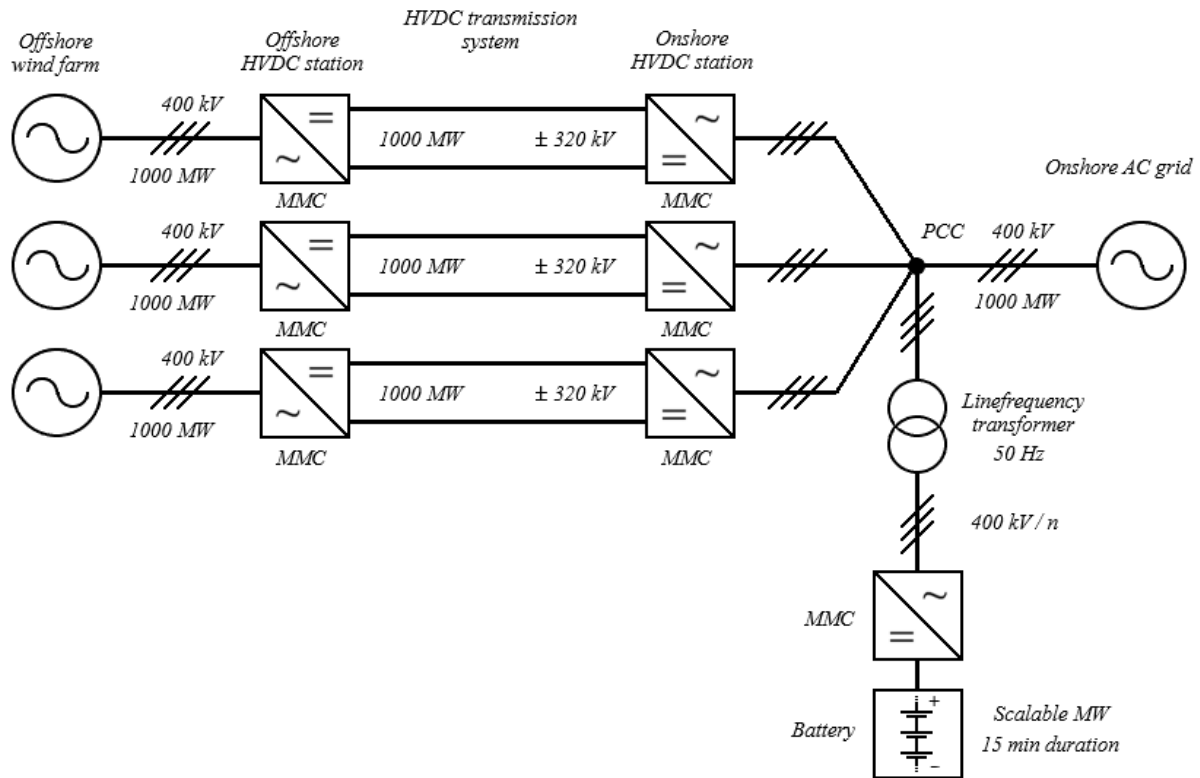


Figure 3.9: Single-line diagram of three HVDC schemes and the MMC-BESS connection

Even if the configuration shown in figure 3.9, may have less possible single point of failures than the MMC-BESS connected to the DC-link, this configuration will highly rely on the integrity of one large MMC-BESS.

Another possibility that may be considered for a stepwise project development with two or more HVDC schemes, would be to connect two or more large MMC-BESS's to the AC-grid side of the onshore converter. This will be a similar approach as for the MMC-BESS connected to the DC-link of the HVDC system, but in this case the Point of Common Coupling (PCC) to the onshore bulk power system will enable the possibility for cross-redundancy as the operating MMC-BESS will not be closely tied to any of the HVDC schemes.

In addition, it may be considered an unequal number of MMC-BESS's compared to the number of HVDC schemes. If two MMC-BESS's are concluded to be sufficient to provide ancillary services for three HVDC schemes, this may reduce the overall cost, due to the reduced number of converters.

This configuration is illustrated in figure 3.10, where two or more MMC-BESS's are connected to the AC grid side of the onshore converter.

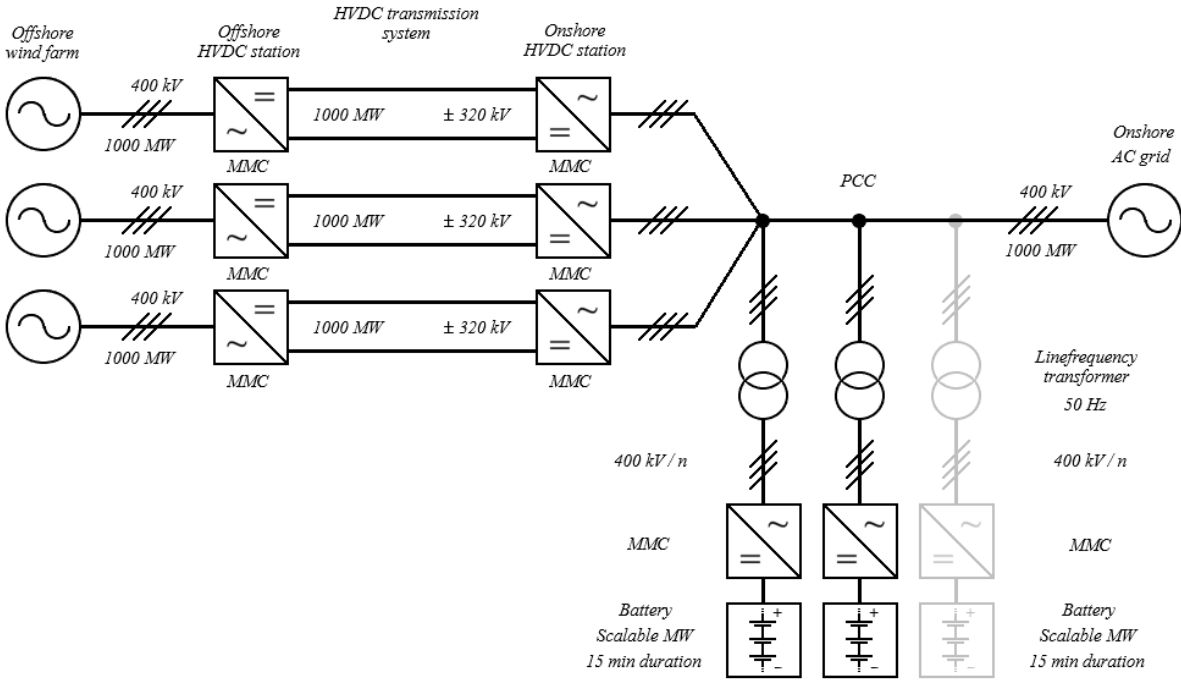


Figure 3.10: Single-line diagram of three HVDC schemes and two or more MMC-BESS's

4 Discussion

In this chapter the discussion of the reviewed literature and the assessed solutions are performed. The assessment in chapter 3 may to a certain extent also be considered as a discussion, but for the sake of a good order, a separate discussion chapter is added.

In chapter 1 the thesis was introduced, the objective and problem statement were described, the SoW and limitations was clarified, and an outline of the thesis was included.

In chapter 2.1 traditional power system stability services are reviewed.

The required amount of active power to rebalance the frequency after a contingency event can be considered to be equal for an IBR and a synchronous generator. Thus, the traditional needs for primary and secondary reserves are found transferrable and dimensioning for the capacity and design of an electrochemical energy storage. Furthermore, a reserve between 15 to 20 % of the base load is recommended.

The present challenges related to RES integration are tied to the geographical location, as smaller and more isolated grids soon will experience a higher percentage of IBR's. The larger interconnected BPS's will have a substantial amount of traditional power sources for the years to come and a contingency event will not make up such a large proportion of the total power generation. However, it may be a risk that smaller parts of the larger interconnected BPS's are disconnected and that IBR's then will cause problems with regards to power system stability. Therefor, it is recommended to assess the BPS in the specific region, when designing the solutions and determining the need of redundancy and robust solutions.

In chapter 2.2 electrochemical energy storage technologies are reviewed.

This review is mainly built on a literature review of newer comparison studies for grid-scale energy storage technologies. Lithium-ion, sodium-sulfur, flow batteries, and lead-acid was selected for further review and assessments.

The lithium-ion battery technology is found to be the most promising candidate, due to its high power density, low cost, high commercially availability and the proven implementation in large scale battery energy storage facilities for power system stabilization.

When assessing the reviewed batteries, sustainability and environmental impacts must be kept in mind. When shifting the traditional power sources to more sustainable sources, by relying on energy storage solutions, it is crucial that these storage technologies also are assessed with regards to sustainability.

It is observed that the lithium-ion technology includes some subcategories. Furthermore, that these subcategories all perform well and are cost competitive. With the sustainability aspect in mind and an objective to reduce the reliance on scarce and rare minerals, the LFP subcategory is identified as a good candidate.

The LFP will reduce the reliance on scarce minerals, compared to the other commercially available lithium-ion chemistries, and the LFP can compete with regards to technical properties and the cost. Therefore, lithium-ion LFP batteries are recommended in this thesis.

In chapter 2.3 HVDC technologies and HVDC systems are reviewed.

It is observed that the only type of commercially available HVDC converters that can comply with the services described in chapter 2.1 is the VSC's. Furthermore, it is in chapter 2.3.4 observed that the only VSC technology presented on the supplier webpages are the MMC, which is considered to be the state-of-the-art of the VSC's.

This observation may be an indication of that other VSC's, like the 2L-VSC's, are considered to be obsolete. Therefore, it is concluded that the most relevant converter technology for the HVDC scheme in this thesis will be the VSC MMC technology.

In chapter 2.3.5, some reference HVDC projects were reviewed.

The capacity and DC-link voltage of comparable HVDC projects for offshore wind farms, gives a clear indication of the foreseen capacity and voltage levels. The DC link voltage for the project in this thesis can be estimated to be equal to 320 kV DC and the power capacity can be estimated to be equal to 1000 MW.

A reserve for primary and secondary services, of 15 to 20 % of the base load will then be equal to 150 to 200 MW, when considering a HVDC scheme equal to 1000 MW. To comply with the requirements for secondary control functionalities, the reserve must sustain a power flow at maximum output level for at least 10 minutes. To have some headroom and to avoid

deep-cycling of the batteries, it is recommended that the energy storage should sustain a discharge at rated output power for 15 minutes.

In chapter 2.4 BESS technologies, commercially available solutions and reference projects were reviewed. Followed by a review of two master theses describing the utilization of HVDC-BESS's, a connection to the DC-link of a HVDC system, and a connection to the onshore BPS, in chapter 2.5.

It is observed that the commercially available BESS solutions have proven their functionalities and capabilities. Furthermore, that is has been commissioned reference projects, where large scale BESS's are used for power system stability purposes. The power capacity for some of these reference projects, exceed the needed power capacity for the usage intended and assessed in this thesis.

The MMC-BESS's has not yet been identified in any reference project. However, the literature and the availability of components and building blocks are indicating that this should be feasible to realize. These MMC-BESS configurations do come with some considerations.

If an MMC-BESS is connected to the DC-link of the HVDC system, the ancillary services will be fully dependent of the availability of both the MMC-BESS converter and the onshore HVDC converter. A single-point-of-failure may cause an outage of the ancillary service. This may be considered acceptable, if the MMC-BESS is meant to only provide ancillary service for this specific HVDC scheme.

If the offshore wind farm is operated at maximum rated power and a contingency event occurs in the onshore BPS, the active power from the BESS, needs to flow through the onshore HVDC converter. If the system should provide ancillary services when operating at rated wind power capacity, the dimensioning of the onshore converter must be considered.

In case a stepwise expansion of the project and offshore wind farm is considered, where one or more new HVDC schemes will be added, and which is a practice that are identified among the reference projects, MMC-BESS's must be connected to the DC-link of each HVDC scheme to ensure full availability.

The connection to the DC link may be promising for future “hybrid cable” multiterminal HVDC schemes, providing power to more than one onshore station.

The MMC-BESS connected to the DC-link of the HVDC system, will require at least two converters in a DC/AC/DC configuration to be able to adjust the voltage levels towards the battery packages connected in serial and in parallel.

If an MMC-BESS is connected to the AC-grid side of the onshore converter, it will be sufficient with one AC/DC converter connected towards the battery packages. However, if using only one AC/DC MMC, it will not be possible to adapt deep cycling, since the DC voltage must be higher than the AC amplitude.

The MMC-BESS connected to the AC-grid side of the onshore HVDC converter will not rely on the onshore HVDC converter itself and would therefore have less possible single-point-of-failures that may result in an outage of the ancillary services. This may not be considered relevant, if the ancillary services only should be used for this specific HVDC scheme, but in case other HVDC schemes or RES should rely on this MMC-BESS, it would be an advantage.

If three HVDC schemes are considered, two large MMC-BESS’s connected to the onshore AC-grid side, may be sufficient, as these will not rely on the HVDC schemes itself, and as the cross-redundancy of having two independent MMC-BESS’s may be concluded sufficient.

Although the MMC-BESS’s are possible to realize, with regards to availability of technology and components, it has not yet been realized, tested, or commissioned. Therefore, it may be premature to conclude on such a solution for projects in the very near future.

The commercially available BESS’s have proven their feasibilities and their matureness with regards to deployment and operation. This will be a safe option with regards to project execution and to reduce risks of schedule impact. In addition, these solutions are highly scalable, impose redundancy, availability, and maintainability, as they are consisting of several units.

Reference projects has as mentioned, and reviewed in chapter 2.4.3, been identified and where the capacity of the plant is exceeding the need for this project and were the services provided are transferrable to this project. This proves the readiness of existing commercially available BESS’s to be implemented in the nearest future.

However, these large BESS plants are consisting of hundreds of BESS units to make up a reserve of hundreds of MW's. This type of BESS technology would require a significant amount of individual BESS units and LV/MV/HV transformers to make up for the displacement of traditional energy sources in the larges interconnected BPS's.

Therefore, it may be a naturally technology development that the BESS units also become bigger, at least that it appears some alternatives with bigger units. The existing MMC-HVDC technology may then be a natural option to consider for such a development of commercially available large scale BESS's.

For offshore wind HVDC projects to be realized in the nearest future, it is recommended to use a commercially available BESS solution, to connect this BESS-plant to the onshore AC bulk power system and if available from the manufacturer, to use the LFP lithium-ion chemistry for the battery packages.

5 Conclusion

In this thesis, solutions for large-scale power system stability services, has been reviewed and assessed. More specifically, an electrochemical energy storage is intended to provide ancillary services of primary and secondary reserves for an HVDC scheme connected to a large-scale offshore wind farm.

Literature is reviewed and assessed. Both for identifying the need and the possible solutions.

Technology candidates for electrochemical energy storage are reviewed and assessed. The main parameters of selection will be power capacity, cost range with respect to power capacity, power and energy density, response time, the matureness of commercialization and the reliance of scarce minerals.

The lithium-ion battery technology has been selected as the preferred electrochemical storage candidate. This due to its excellent performances with regards to power capacity, the widely commercialization and examples of deployments for ancillary services, and the relatively low cost. Furthermore, the subcategory LFP has been selected as the preferred lithium-ion chemistry. This to reduce the reliance on scarce minerals in combination with that LFP is considered to increase its market shares significantly during the coming decade.

For the BESS, the preferred solution, as of today, will be to use a commercially available BESS solution connected to the AC grid side of the onshore converter. Both as this technology is commercially available and as it has been commissioned plants, that exceeds the requirements for the example HVDC scheme used in this thesis. The large-scale power stability services have proven their functionalities and the project risk is deemed to be lower than for the alternatives.

However, as the technology development is evolving rapidly, it is strongly recommended to continuously review new literature and to assess new possibilities. Both with regards to electrochemical storage technologies and with regards to BESS converter topologies – and specially the utilization of MMC HVDC BESS's.

6 Further Work

It is recommended to continue the review and assessment of electrochemical energy storage technologies and the BESS converter technologies with respect to large-scale plants.

The battery technology is evolving rapidly, and what seems to be the most promising technology for the decades to come, may change within the first years to come.

The development of lithium-air batteries and solid-state lithium-ion batteries should be followed closely. In addition, the development of other battery technologies, like the sodium-sulfur, should be closely followed, as some of the technical constraints and cost aspect may change significantly within short time. It may also appear new battery technologies which are not yet known.

The number of commercially available BESS solutions has increased rapidly in the most recent years, but the low voltage level and the high number of units and transformers required to create a large plant, seems to be a common denominator. Larger BESS units may be a promising field for further research and development.

The utilization of commercially available MMC-HVDC converters to create large-scale MCC-BESS's is an interesting and promising field of study. If a large amount of the traditional power sources in the bulk power system is to be displaced by inverter-based resources, it would require a significant amount of traditional BESS inverter packages. Bigger MMC-BESS's may be cost competitive if deployed to a such extent that economies of scale are achieved. Therefore, this is recommended to be followed-up further.

The utilization of distributed batteries in an MMC has not be reviewed, explained, or assessed in this thesis. It is recommended to review this concept.

Any connection to the DC-link of the HVDC system must be assessed with regards to protection coordination and the need of DC-breakers, as this configuration will act as a multiterminal HVDC scheme.

When locating IBR's close to each other, e.g., onshore HVDC converters, it may cause issues in form of negative- or harmonic control interaction between the converters. This

phenomenon is not considered in this thesis and in-depth analysis would be required if locating HVDC converters close to each other's.

Substantial Dynamic Performance Studies (DPS) must be performed to clarify and understand the dynamic behavior between converters when fault scenarios occur. E.g., asymmetrical faults, phase-ground faults and more.

In further studies, other energy storage technologies than electrochemical may also be considered. E.g., supercapacitors, compressed air energy systems, pumped-storage hydroelectric, flywheels, ammonia, hydrogen and more.

References

- [1] NERC, 2021 May 11. [Internet]. *Balancing and Frequency Control Reference Document Prepared by the NERC Resources Subcommittee*. Technical Report, North American Electric Reliability Corporation. [cited 2022 February 17]. Available from: https://www.nerc.com/comm/OC/ReferenceDocumentsDL/Reference_Document_NERC_Balancing_and_Frequency_Control.pdf
- [2] Denholm, Paul, Trieu Mai, Rick Wallace Kenyon, Ben Kroposki, and Mark O'Malley. 2020. [Internet]. *Inertia and the Power Grid: A Guide Without the Spin*. Golden, CO: National Renewable Energy Laboratory. [cited 2022 January 21]. NREL/TP-6120-73856. Available from: <https://www.nrel.gov/docs/fy20osti/73856.pdf>
- [3] Luo W., Stynski S., Chub A., Franquelo L. G., Malinowski M., Vinnikov D., *Utility-Scale Energy Storage Systems; A Comprehensive Review of Their Applications, Challenges, and Future Directions*. IEEE Industrial Electronics Magazine. 2021 January 6. doi: 10.1109/MIE.2020.3026169. p. 17-27.
- [4] Lin, Yashen, Joseph H. Eto, Brian B. Johnson, Jack D. Flicker, Robert H. Lasseter, Hugo N. Villegas Pico, Gab-Su Seo, Brian J. Pierre, and Abraham Ellis. 2020. [Internet] *Research Roadmap on Grid-Forming Inverters*. Golden, CO: National Renewable Energy Laboratory. [cited 2022 January 21]. NREL/TP-5D00-73476. Available from: <https://www.nrel.gov/docs/fy21osti/73476.pdf>
- [5] Matevosyan J., MacDowell J., Miller N., Badrzadeh B., Ramasubramanian D., Isaacs A., Quint R., Quitmann E., Pfeiffer R., Urdal H., Prevost T., Vittal V., Woodford D., Huang S. H., O'Sullivan J., *A Future With Inverter-Based Resources; Finding Strength From Traditional Weakness*. IEEE Power & Energy Magazine. Nov./Dec. 2021. doi: 10.1109/MPE.2021.3104075. p. 18-28.
- [6] Matevosyan J., MacDowell J., Miller N., Badrzadeh B., Ramasubramanian D., Isaacs A., Quint R., Quitmann E., Pfeiffer R., Urdal H., Prevost T., Vittal V., Woodford D., Huang S. H., O'Sullivan J., *A Future With Inverter-Based Resources; Finding Strength From Traditional Weakness*. IEEE Power & Energy Magazine. Nov./Dec. 2021. doi: 10.1109/MPE.2021.3104075. *Figure 1. The basic traits and grid services of GFL IBRs, GFM IBRs, and synchronous machines*; p. 21.
- [7] Lin, Yashen, Joseph H. Eto, Brian B. Johnson, Jack D. Flicker, Robert H. Lasseter, Hugo N. Villegas Pico, Gab-Su Seo, Brian J. Pierre, and Abraham Ellis. 2020. *Research Roadmap on Grid-Forming Inverters*. Golden, CO: National Renewable Energy Laboratory. NREL/TP-5D00-73476. *Table 1, Comparison of Grid-Following and Grid-Forming Controls*; p. 10. Available from: <https://www.nrel.gov/docs/fy21osti/73476.pdf>

- [8] Matevosyan J., MacDowell J., Miller N., Badrzadeh B., Ramasubramanian D., Isaacs A., Quint R., Quitmann E., Pfeiffer R., Urdal H., Prevost T., Vittal V., Woodford D., Huang S. H., O’Sullivan J., *A Future With Inverter-Based Resources; Finding Strength From Traditional Weakness*. IEEE Power & Energy Magazine. Nov./Dec. 2021. doi: 10.1109/MPE.2021.3104075. *Figure S1, Power generation and grid support technologies. SVC: static var compensator; STATCOM: static synchronous compensator; p. 20.*
- [9] Wikimedia Commons. File:Wide area synchronous grid (Eurasia, Mediterranean).png. Wikipedia; Alinor. Updated 2022 March 16th Source: [https://commons.wikimedia.org/wiki/File:Wide_area_synchronous_grid_\(Eurasia,_Mediterranean\).png](https://commons.wikimedia.org/wiki/File:Wide_area_synchronous_grid_(Eurasia,_Mediterranean).png). License information: <https://creativecommons.org/licenses/by-sa/3.0/deed.en>
- [10] Lin, Yashen, Joseph H. Eto, Brian B. Johnson, Jack D. Flicker, Robert H. Lasseter, Hugo N. Villegas Pico, Gab-Su Seo, Brian J. Pierre, and Abraham Ellis. 2020. *Research Roadmap on Grid-Forming Inverters*. Golden, CO: National Renewable Energy Laboratory. NREL/TP-5D00-73476. Figure 9, Total annual and instantaneous inverter-based wind and solar generation based on power system size; p. 32. Available from: <https://www.nrel.gov/docs/fy21osti/73476.pdf>
- [11] Bowen, Thomas, Ilya Chernyakhovskiy, Kaifeng Xu, Sika Gadzanku, and Kamyria Coney. 2021. [Internet]. *USAID GRID-SCALE ENERGY STORAGE TECHNOLOGIES PRIMER*. Golden, CO: National Renewable Energy Laboratory. [cited 2022 April 1]. NREL/TP-6A20-76097. Available from: <https://www.nrel.gov/docs/fy21osti/76097.pdf>
- [12] Lin, Yashen, Joseph H. Eto, Brian B. Johnson, Jack D. Flicker, Robert H. Lasseter, Hugo N. Villegas Pico, Gab-Su Seo, Brian J. Pierre, and Abraham Ellis. 2020. *Research Roadmap on Grid-Forming Inverters*. Golden, CO: National Renewable Energy Laboratory. NREL/TP-5D00-73476. *Figure 11, Incorporating grid-forming (GFM) controls into the bulk electric grid will take place gradually after key functionalities have been demonstrated and confidence has been gained by operating them in smaller microgrids and island power systems; p. 35.* Available from: <https://www.nrel.gov/docs/fy21osti/73476.pdf>
- [13] Wikimedia Commons. File:ElectrochemCell.png. Wikipedia; user; Alksub, 2006 June 1. Source: <https://commons.wikimedia.org/wiki/File:ElectrochemCell.png>. License: https://commons.wikimedia.org/wiki/Commons:GNU_Free_Documentation_License,_version_1.2
- [14] Wikimedia Commons. File:Ragone-Diagramm.svg. Wikipedia; user; FelixFliX, 2015 July 19. Source: <https://commons.wikimedia.org/wiki/File:Ragone-Diagramm.svg>. License: <https://creativecommons.org/licenses/by-sa/4.0/deed.en>

- [15] Mongird, K., Viswanathan, V., Alam J., Vartanian C., Sprenkle V., Baxter R., 2020. [Internet]. *2020 Grid Energy Storage Technology Cost and Performance Assessment*. Richland, WA: Pacific Northwest National Laboratory. [cited 2022 April 10]. Technical Report DOE/PA-0204. Available from: [Final - ESGC Cost Performance Report 12-11-2020.pdf \(pnnl.gov\)](#)
- [16] Bowen, Thomas, Ilya Chernyakhovskiy, Kaifeng Xu, Sika Gadzanku, and Kamyria Coney. 2021. *USAID GRID-SCALE ENERGY STORAGE TECHNOLOGIES PRIMER*. Golden, CO: National Renewable Energy Laboratory. NREL/TP-6A20-76097. *Table 1, Qualitative Comparison of Energy Storage Technologies; p. 3.* <https://www.nrel.gov/docs/fy21osti/76097.pdf>
- [17] Bowen, Thomas, Ilya Chernyakhovskiy, Kaifeng Xu, Sika Gadzanku, and Kamyria Coney. 2021. *USAID GRID-SCALE ENERGY STORAGE TECHNOLOGIES PRIMER*. Golden, CO: National Renewable Energy Laboratory. NREL/TP-6A20-76097. *Table 2, Comparison of Electrochemical Storage Technologies; p. 6.* <https://www.nrel.gov/docs/fy21osti/76097.pdf>
- [18] Wikimedia Commons. File:Lithium Iron Phosphate LiFePO4 Cells 700Ah in Parallel and Series and Busbar - 1.jpg. Wikipedia; user; Yo-Co-Man, 2017 August 14. Source: https://commons.wikimedia.org/wiki/File:Lithium_Iron_Phosphate_LiFePO4_Cells_700Ah_in_Parallel_and_Series_and_Busbar_-_1.jpg. License: <https://creativecommons.org/licenses/by-sa/4.0/deed.en>
- [19] Bowen, Thomas, Ilya Chernyakhovskiy, Kaifeng Xu, Sika Gadzanku, and Kamyria Coney. 2021. *USAID GRID-SCALE ENERGY STORAGE TECHNOLOGIES PRIMER*. Golden, CO: National Renewable Energy Laboratory. NREL/TP-6A20-76097. *Table 4, Operating Characteristics of Select Lithium-Ion Chemistries; p. 9.* <https://www.nrel.gov/docs/fy21osti/76097.pdf>
- [20] Neoen. Hornsdale Power Reserve [Internet]. Canberra: Neoen; 2021. [Cited 2022 April 16]. Available from: <https://hornsdalepowerreserve.com.au/>
- [21] Neoen. Victorian Big Battery [Internet]. Canberra: Neoen; 2021. [Cited 2022 April 16]. Available from: <https://victorianbigbattery.com.au/>
- [22] Wikimedia Commons. File:Li-air-charge-discharge.jpg. Wikipedia; user; Na9234. Source: <https://commons.wikimedia.org/wiki/File:Li-air-charge-discharge.jpg>. License information: <https://creativecommons.org/licenses/by/3.0/deed.en>
- [23] Wikimedia Commons. File:NaS battery en.svg. Original = NASA John Glenn Research Center, Vector: Sandra Hanbo, 2012 January 20. Source: https://commons.wikimedia.org/wiki/File:NaS_battery_en.svg. License: <https://creativecommons.org/licenses/by-sa/4.0/deed.en>
- [24] Bowen, Thomas, Ilya Chernyakhovskiy, Kaifeng Xu, Sika Gadzanku, and Kamyria Coney. 2021. *USAID GRID-SCALE ENERGY STORAGE*

TECHNOLOGIES PRIMER. Golden, CO: National Renewable Energy Laboratory. NREL/TP-6A20-76097. *Table 3, Advantages and Disadvantages of Select Electrochemical Battery Chemistries*; p. 7.

<https://www.nrel.gov/docs/fy21osti/76097.pdf>

- [25] Wikimedia Commons. Redox Flow Battery. Colintheone, 2017 May 17. Source: <https://avs.scitation.org/doi/10.1116/1.4983210> License: <https://creativecommons.org/licenses/by-sa/4.0/deed.en> Available from: https://commons.wikimedia.org/wiki/File:Redox_Flow_Battery.jpg
- [26] Wikimedia Commons. File:1 MW 4 MWh Turner Energy Storage Project in Pullman, WA.jpg. Wikipedia; user; UniEnergy Technologies, 2015 May 22. License: <https://creativecommons.org/licenses/by-sa/4.0/deed.en> Source: https://commons.wikimedia.org/wiki/File:1_MW_4_MWh_Turner_Energy_Storage_Project_in_Pullman_WA.jpg.
- [27] Wikimedia Commons. File:Photo-CarBattery.jpg, 2005 November 5. Source: <https://commons.wikimedia.org/wiki/File:Photo-CarBattery.jpg> . License information: https://en.wikipedia.org/wiki/en:public_domain
- [28] Murname M., Ghazel, A., 2017. [Internet]. *A Closer Look at State of Charge (SOC) and State of Health (SOH) Estimation Techniques for Batteries*. Norwood, MA: Analog Devices. [cited 2022 April 30]. Available from: <https://www.analog.com/media/en/technical-documentation/technical-articles/A-Closer-Look-at-State-Of-Charge-and-State-Health-Estimation-Techniques.pdf>
- [29] Danko M., Adamec, J., Taraba M., Drgona P., 2019. [Internet]. *Overview of batteries State of Charge estimation methods*. Faculty of electrical engineering and information technology, Department of mechatronics and electronics, University of Zilina, Univerzitná 1, Žilina 010 26, Slovakia. ScienceDirect [cited 2022 April 30]. Available from: <https://www.sciencedirect.com/science/article/pii/S2352146519301905>
- [30] Shokooh Far, M. R. “*AC and DC systems interaction-opportunities and challenges of exchanging system services*” 2018. Master’s Thesis, Department of Electric Power Engineering at the Norwegian University of Science and Technology.
- [31] Sharifabadi, K., Harnefors, L., Nee, H.-P., Teodorescu, R., Norrga, S., 2016. *Design, Control and Application of Modular Multilevel Converters for HVDC Transmission Systems*. John Wiley & Sons.
- [32] Wikimedia Commons. Modular Multi Level Converter. Clampower, 2012 December 1. Clampower, 2012 December 3. License: <https://creativecommons.org/licenses/by-sa/3.0/deed.en> , Source: https://commons.wikimedia.org/wiki/File:Modular_Multi_Level_Converter.png

- [33] Wikimedia Commons. Modular Multi Level Converter submodule states. Clampower, 2012 December 3. License: <https://creativecommons.org/licenses/by-sa/3.0/deed.en> Source:https://commons.wikimedia.org/wiki/File:Modular_Multi_Level_Converter_submodule_states.png
- [34] Siemens Energy. *High-Voltage Direct Current (HVDC) Transmission Solutions*. [Internet]. [Accessed 2022.02.27]. Accessible: <https://www.siemens-energy.com/global/en/offerings/power-transmission/portfolio/high-voltage-direct-current-transmission-solutions.html>
- [35] Hitachi Energy. *HVDC*. [Internet]. [Accessed 2022.02.27]. Accessible: <https://www.hitachienergy.com/offering/product-and-system/hvdc>
- [36] GE Grid Solutions. *HVDC Systems*. [Internet]. [Accessed 2022.02.27]. Accessible: <https://resources.gegridsolutions.com/hvdc>
- [37] Sharifabadi, K., Harnefors, L., Nee, H.-P., Teodorescu, R., Norrga, S., 2016. Design, Control and Application of Modular Multilevel Converters for HVDC Transmission Systems. John Wiley & Sons. Table 7.1, List of TenneT's offshore MMC-HVDC schemes for the export of wind energy to mainland network; p. 284.
- [38] Dogger Bank Wind Farm. *About the project*. [Internet]. [Accessed 2022.04.24]. Accessible: <https://doggerbank.com/about/>
- [39] Sofia Offshore Wind Farm. *About Sofia Offshore Wind Farm*. [Internet]. [Accessed 2022.05.17]. Accessible: <https://sofiawindfarm.com/about/>
- [40] Bayo-Salas, A., Beerten, J., Rimez, J., Van Hertem, D., 2015. [Internet] *Analysis of control interactions in multi-infeed VSC HVDC connections*. IET Gener. Transm. Distrib., 2016, Vol. 10, Iss. 6, pp. 1336–1344. [accessed 2022 May 17]. doi: 10.1049/iet-gtd.2015.0876. Available from: <https://ietresearch.onlinelibrary.wiley.com/doi/epdf/10.1049/iet-gtd.2015.0876>
- [41] Hestad Ø., Tande J. O. “Hybrid cables” explained. [Internet]. Trondheim: SINTEF; #SINTEFblog; 2022 [Accessed 2022.05.17]. Accessible from: <https://blog.sintef.com/sintefenergy/hybrid-cables-explained/>
- [42] Hellesnes, M. N., June 2017. “*Use of Battery Energy Storage for Power Balancing in a Large-Scale HVDC Connected Wind Power Plant*”. Master’s Thesis, Department of Electric Power Engineering at the Norwegian University of Science and Technology.
- [43] Reite, I. P. “*Battery energy storage connected to a three-phase 50 Hz grid*”, 2017. Master’s Thesis, Department of Electric Power Engineering at the Norwegian University of Science and Technology.
- [44] Wikimedia Commons. File:Overhead View of Tehachapi Energy Storage Project, Tehachapi, CA.png. Sandia National Laboratories, 2015 June 1. License: <https://creativecommons.org/publicdomain/mark/1.0/deed.en> Source:

<https://www.sandia.gov/ess-ssl/publications/SAND2015-5242.pdf>. Available from:
https://commons.wikimedia.org/wiki/File:Overhead_View_of_Tehachapi_Energy_Storage_Project,_Tehachapi,_CA.png

- [45] Siemens Energy. *Battery energy storage*. [Internet]. [Accessed 2022.04.24]. Accessible: <https://www.siemens-energy.com/global/en/offerings/storage-solutions/battery-energy-storage.html>
- [46] Hitachi Energy. *e-mesh™ PowerStore™*. [Internet]. [Accessed 2022.04.24]. Accessible: <https://www.hitachienergy.com/offering/solutions/grid-edge-solutions/our-offering/e-mesh/powerstore>
- [47] GE Renewable Energy. *Energy Storage - GE's Reservoir Solutions*. [Internet]. [Accessed 2022.04.25]. Accessible: <https://www.ge.com/renewableenergy/hybrid/battery-energy-storage>
- [48] Fluence. *Fluence Gridstack™*. [Internet]. [Accessed 2022.04.25]. Accessible: <https://fluenceenergy.com/energy-storage-technology/gridstack-grid-energy-storage/>
- [49] Tesla. *Megapack Massive Energy Storage*. [Internet]. [Accessed 2022.04.25]. Accessible: <https://www.tesla.com/megapack>
- [50] Tesla. *Utilities*. [Internet]. [Accessed 2022.04.25]. Accessible: <https://www.tesla.com/utilities>
- [51] FlexGen. *FLEXGEN UTILITY SCALE*. [Internet]. [Accessed 2022.04.25]. Accessible: <https://flexgen.com/utility/>
- [52] Wärtsilä. *Energy Storage & Optimisation*. [Internet]. [Accessed 2022.04.25]. Accessible: <https://www.wartsila.com/energy/solutions/energy-storage>
- [53] Powin. *INTRODUCING THE POWIN CENTIPEDE™ PLATFORM*. [Internet]. [Accessed 2022.04.25]. Accessible: <https://powin.com/products/hardware/>
- [54] LG Energy Solution Vertech. *Energy Storage Solutions For A Brighter World*. [Internet]. [Accessed 2022.04.25]. Accessible: <https://lgensol-vt.com/>
- [55] LG Energy Solution Vertech. *The Battery Storage System Unlike Any Other*. [Internet]. [Accessed 2022.04.25]. Accessible: <https://lgensol-vt.com/solutions/hardware-details/>
- [56] SMA Sunbelt Energy. *Energy experts for innovative projects*. [Internet]. [Accessed 2022.04.25]. Accessible: <https://www.sma-sunbelt.com/>
- [57] Sungrow. *Utility Storage System*. [Internet]. [Accessed 2022.04.25]. Accessible: <https://en.sungrowpower.com/solutionsDetail/11>

- [58] Nidec. *BATTERY ENERGY STORAGE SOLUTIONS*. [Internet]. [Accessed 2022.04.25]. Accessible: <https://www.nidec-industrial.com/markets/battery-energy-storage-solutions/>
- [59] NGK Insulators. *NAS Batteries*. [Internet]. [Accessed 2022.04.25]. Accessible: <https://www.ngk-insulators.com/en/product/nas.html>

